JMA/WMO Workshop on Quality Management of Surface Observations
RA II WIGOS Project
Tokyo, Japan, 19-23 March 2018

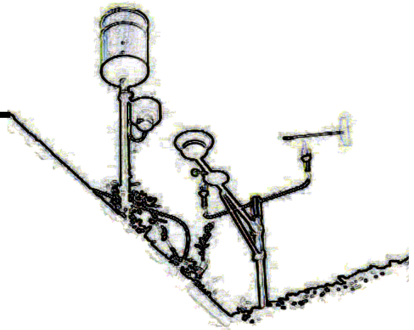

Accuracy of precipitation measurements, instrument calibration and techniques for data correction and interpretation

WIND INDUCED UNDERCATCH:
Field observations and Computational Fluid Dynamics simulations

Tokyo, 22 March 2018

University of Genova - DICCA
Dept of Civil, Chemical and Environmental Engineering

Arianna Cauteruccio
Mattia Stagnaro
Luca G. Lanza

LC-PrIn B. Castelli

WMO/CIMO Lead Centre “B. Castelli” on Precipitation Intensity

WMO

Problem statement & Objective

Wind is recognized as the first environmental source for the undercatch of solid and liquid precipitation as experienced by **catching type gauges**.

The airflow surrounding any precipitation gauge is deformed by the presence of the gauge body, resulting in the acceleration of wind above the orifice of the instrument, which deflects the hydrometeors (liquid/solid particles) away from the collector (the wind induced undercatch).

Casella tipping bucket rain gauge

Geonor T200B weighing rain gauge

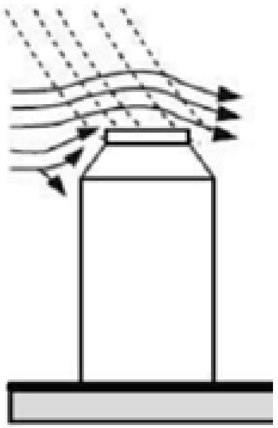

Airflow above the collector of a shielded rain gauge

The undercatch depends on:

- rain gauge geometry
- wind speed
- type of precipitation: **rain** or **snow**
- precipitation intensity

→ Aerodynamic response / generated turbulence

→ Drag coefficient / trajectories

Drop size distribution (DSD)

Hardware solutions

Wind shield

Single Alter wind shield

Aerodynamic rain gauge

EML tipping bucket rain gauges

Scientific research

Field data analysis

WMO Reference

Rain gauges in operational conditions

Numerical simulations

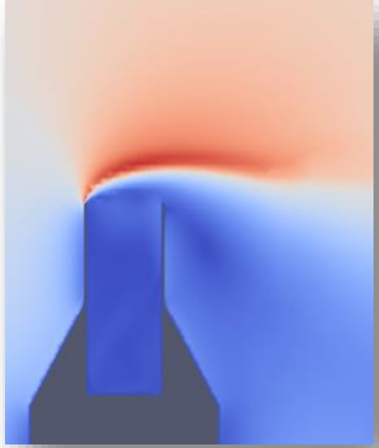

Airflow

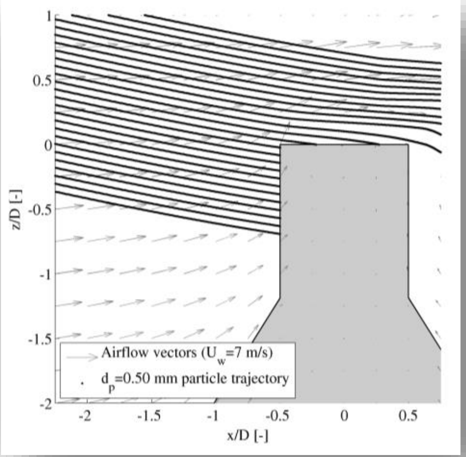

Droplet trajectories

Overall objective: Derive suitable correction curves (transfer functions) for operational use

Section 1

Field observation:
STATE OF THE ART

WMO

SPICE Solid Precipitation
Inter-Comparison Experiment

Field Observations

Three years 2011-2013, about 20 field sites e.g:

- Marshall (Colorado)
- Haukeliseter (Norwey)
- Formigal (Spain)
- Weissfluhjoch (Switzerland)
- Joetsu (Japan)
- …

h_{mis}

Instruments in operational conditions

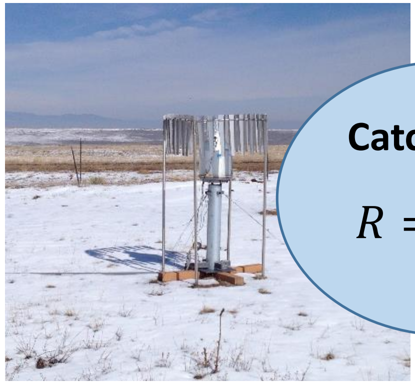

Catch Ratio

$$R = \frac{h_{mis}}{h_{ref}}$$

h_{ref}

Double Fence Inter-comparison Reference (DFIR) - WMO

Marshall (CO), Geonor T200B unshielded and with single Alter wind shield.

Marshall (CO)

Thériault et al. 2015

This study shows that even the DFIR measurements are affected by wind depending on the orientation of the DFIR related to wind direction. The analysis was conducted by means of the airflow CFD simulation around the DFIR and the particles tracking model.

The DFIR is octagonal therefore two different orientation were tested.

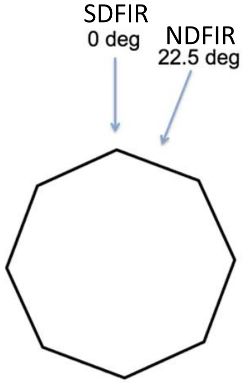

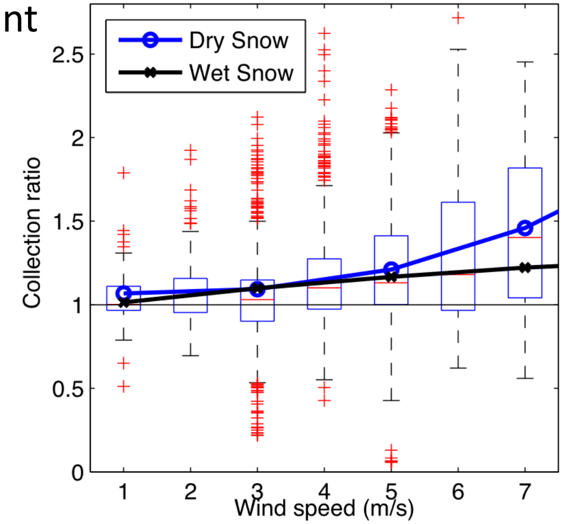

Collection ratio:

$$R = \frac{h_{SDFIR}}{h_{NDFIR}} \neq 1$$

Line:
numerical results.
Boxplot:
experimental observations at Marshall site.

Haukeliseter (Norway) experimental site

- Data from three winters (2011-2013)
- Wind measurements at 10 m height (WMO standard) and gauge height
- Temperature measurements

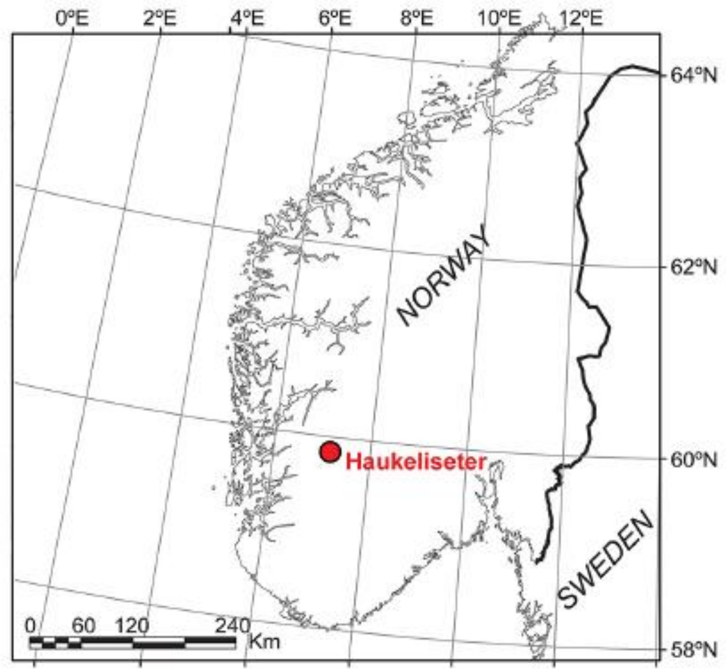

$$R = \frac{h_{mis}}{h_{ref}}$$

h_{mis} → Geonor T200B with a single alter wind

h_{ref} → DFIR

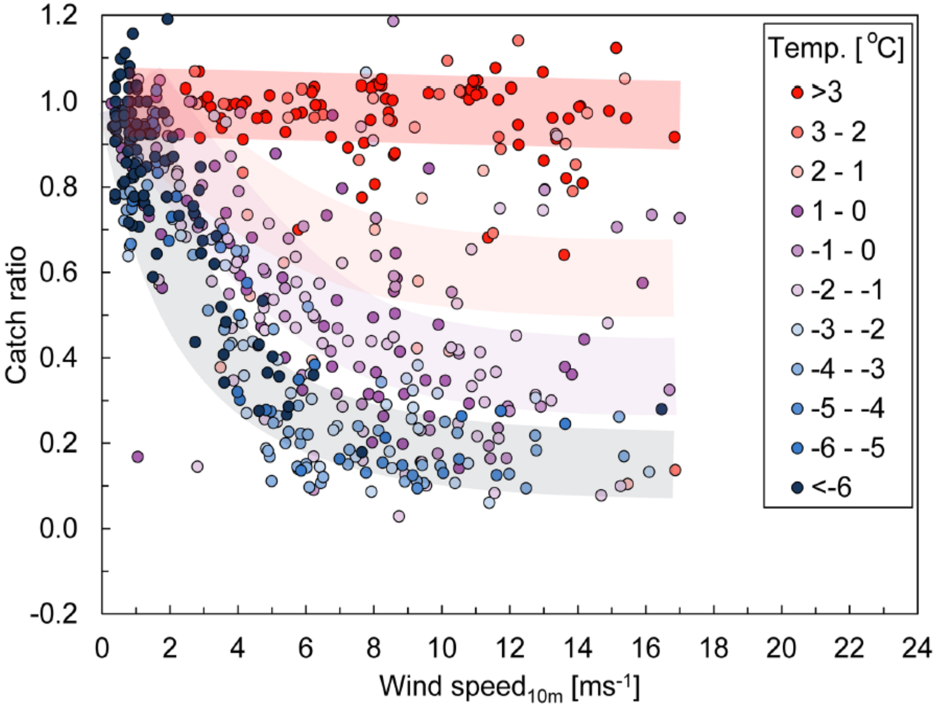

Temperature and type of precipitation:

T≥2°C rain	Catch ratio is not influenced significantly by the wind
-2<T<2 °C mixed	liquid/solid → DSD → Large scatter of data
T≤-2 °C snow	Characteristic decreasing shape

Objective: derive a new *adjustment function* to obtain the real precipitation from the measured one

Ref.: Wolff M.A. et al. (2015)

"Adjustment" function used in Norway

Existing "Adjustment" Function, *Førland et al. (1996)*

- For Geonor gauge
- Cold climate in Nordic country

SOLID precipitation

$$p_T = p_M g_1(V,T) = p_M e^{(b_0 + b_1 V + b_2 T + b_3 V T)}$$

- p_T true precipitation
- p_M measured precipitation
- T air temperature
- V wind speed at the gauge high
- b0, b1,b2,b3 parameters

LIQUID precipitation

$$p_T = p_M g_2(V,T) = p_M e^{[c_0 + c_1 V + c_2 \log(I) + b_3 V \log(I)]}$$

- Function of the precipitation Intensity I → Wide spectrum of different precipitation events

I is used an indirect measure of drop size DSD

New "Adjustment" Function, *Wolff M.A. et al. (2015)*

Dependence of temperature

$$p_T = \begin{cases} p_M g_1(V,T) & T \leq 0.0°\mathrm{C} \\ p_M \{g_1(V,T) + g_2(V,I)\}/2 & 0.0 < T \leq 2.0°\mathrm{C} \\ p_M g_2(V,I) & T > 2.0°\mathrm{C}. \end{cases}$$

→ MIXED precipitation

Problem of this formulation:
The lack of continuity when the temperature varies across the limits during an event.

Adjustment function used in Norway

New Adjustment Function, *Wolff M.A. et al. (2015)*

1. Initial criteria:
- The catch ratio is function of wind speed V only
- The ratio decreases exponentially as a function of V

$$R|T = \frac{p_M}{p_T} = (1-\tau)\, e^{-\left(\frac{V}{\theta}\right)^{\beta}} + \tau$$

2. Assumption:
- The catch ratio varies with temperature T

$$R = f(V,T) = [1-\tau(T)]\, e^{-\left[\frac{V}{\theta(T)}\right]^{\beta(T)}} + \tau(T)$$

3. Assumption:
- The parameter functions are described by sigmoid function

$$\phi(T) = \phi_1 + (\phi_2 - \phi_1)\frac{e^{(T-T_\phi)/s_\phi}}{1+e^{(T-T_\phi)/s_\phi}}$$

4. Bayesian Model Likelihood (BML)
- the parameters θ and β are constant
- τ=τ(T)

$$R_i = \left[1 - \tau_1 - (\tau_2 - \tau_1)\frac{e^{\left(\frac{T_i - T_\tau}{s_\tau}\right)}}{1+e^{\left(\frac{T_i - T_\tau}{s_\tau}\right)}}\right] e^{-\left(\frac{V_i}{\theta}\right)^{\beta}} + \tau_1 + (\tau_2 - \tau_1)\frac{e^{\left(\frac{T_i - T_\tau}{s_\tau}\right)}}{1+e^{\left(\frac{T_i - T_\tau}{s_\tau}\right)}} + \sigma(T_i)\,\varepsilon_i,$$

τ_i, S_τ, T_τ differs for wind speed measures a 10m or at gauge height (4,5m).

This function ensures the required continuity across a wide range of temperature.

Results:
A continuous equation which describes the wind–induced undercatch for snow, mixed precipitation and rain events for wind speed up to 20m/s and temperature up to 3°C.

Adjustment function used in Norway

It is recommended to use the wind data at the gauge height wherever possible!

But

the aerodynamic effect of other nearby installation must be taken into account.

The large data set allows to derive the adjustment function and to test it with other events.

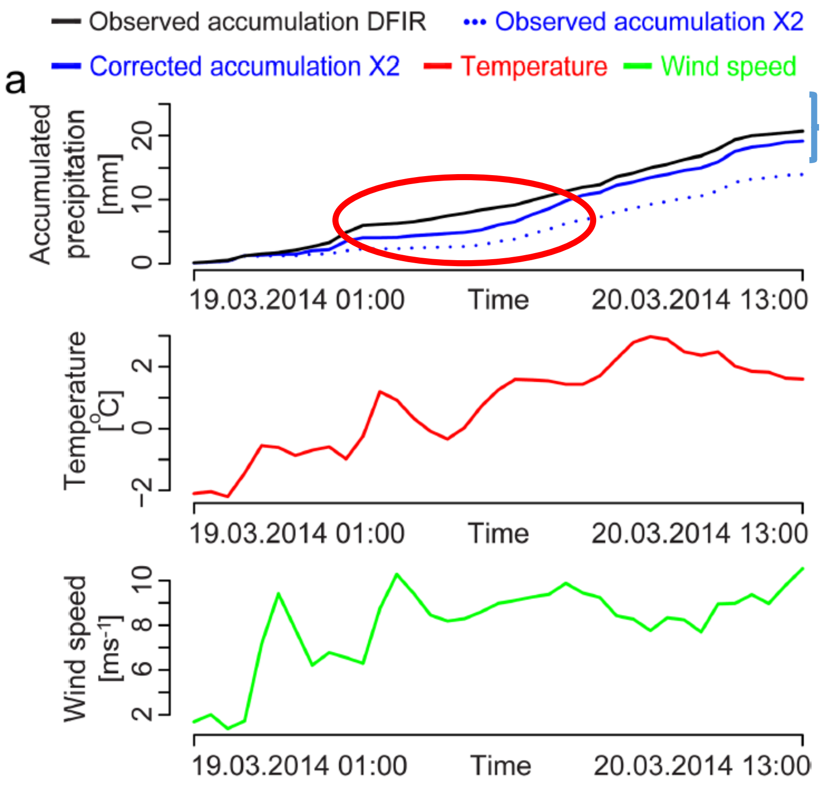

DSD?

Norway and USA experimental sites

Exponential transfer Function, *Kochendorfer et al. (2017a)*

- Data from the winter (2010) (Before SPICE)
- Two sites: Marshall (USA) and Haukeliseter (NOR)
- Temperature measurements

Haukeliseter

- Wind measurements at 10 m and 4.5 m
- 4.5 m gauges collectors height

↓

Evaluation of shadowing $U_{4.5m} = 0.93U_{10m}$

Marshall

- Wind measurements at 10 m
- 1.9 m gauges collectors height

↓

$U_z \approx \ln\left[(z-d)/z_0\right]$ Uz wind speed at a height z
z_0=0.01 m roughness length
d= 0.4m displacement length

$$U_{1.9m} = 0.71U_{10m}$$

GAUGES:

- DFRIR (USA and NOR)
- unshielded (USA and NOR)
- Single Alter (USA and NOR)
- Double Alter (USA)
- Belfort Double Alter (USA)
- Small DFIR (USA)

Haukeliseter

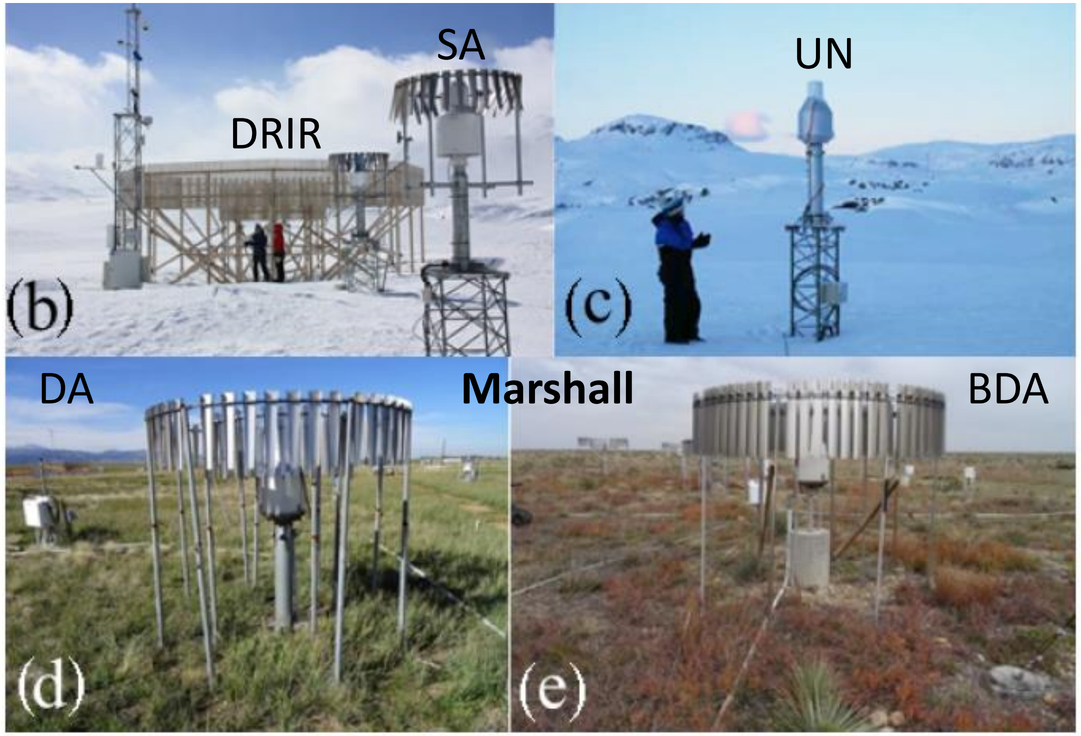

Existing Transfer Function, *Wolff M.A. et al. (2015)*

$$\mathrm{CE}=\left[1-\tau_1-(\tau_2-\tau_1)\frac{e^{\left(\frac{T_{\mathrm{air}}-T_\tau}{s_\tau}\right)}}{1+e^{\left(\frac{T_{\mathrm{air}}-T_\tau}{s_\tau}\right)}}e^{-\left(\frac{U}{\theta}\right)^\beta}\right]+\tau_1+(\tau_2-\tau_1)\frac{e^{\left(\frac{T_{\mathrm{air}}-T_\tau}{s_\tau}\right)}}{1+e^{\left(\frac{T_{\mathrm{air}}-T_\tau}{s_\tau}\right)}}$$

Sigmoid response (sig)

New Transfer Function,. *Kochendorfer et al. (2017a)*

$$\mathrm{CE}=e^{-a(U)\left(1-\left[\tan^{-1}(b(T_{\mathrm{air}}))+c\right]\right)}$$

Exponential response (exp)

Gauge height wind speed

Shield	Sig coef						Exp coef			n	Max U
	τ_1	τ_2	T_τ	s_τ	θ	β	a	b	c		$(\mathrm{m\,s^{-1}})$
US UN	0.31	0.94	−0.08	0.92	2.58	1.23	0.063	1.22	0.66	843	6
All SA	0.20	0.96	0.22	1.11	4.70	1.97	0.040	1.10	0.54	1501	9
NOR SA	0.26	1.02	0.88	0.99	3.1	1.61	0.054	0.71	0.26	352	9
US SA	0.16	0.95	−0.34	1.01	4.9	1.90	0.036	1.04	0.63	1156	6
US DA	0.00	0.92	−1.19	1.89	7.04	1.36	0.028	0.74	0.66	1392	6
US BDA	0.00	1.00	1.81	0.57	8.73	2.87	0.015	0.32	0.38	1204	6
US SDFIR	0.99	0.96	0.52	0.10	0.14	6.16	0.006	0.00	0.00	1508	6

10 m wind speed

Shield	Sig coef						Exp coef			n	Max U
	τ_1	τ_2	T_τ	s_τ	θ	β	a	b	c		$(\mathrm{m\,s^{-1}})$
US UN	0.31	0.94	−0.08	0.92	3.58	1.23	0.045	1.21	0.66	843	8
All SA	0.17	0.96	0.23	1.11	6.46	2.01	0.03	1.04	0.57	1501	12
NOR SA	0.25	1.03	0.95	1.06	3.99	1.61	0.05	0.66	0.23	352	12
US SA	0.12	0.95	−0.35	1.01	7.05	1.87	0.03	1.06	0.63	1156	12
US DA	0.00	0.92	−1.19	1.89	9.75	1.36	0.021	0.74	0.66	1392	8
US BDA	0.31	1.00	1.79	0.58	10.0	3.15	0.01	0.48	0.51	1204	8
US SDFIR	0.99	0.96	0.52	0.10	0.14	10.75	0.004	0.00	0.00	1508	8

Different wind speed response compared to DFIR

Analysis of results

Wind speed effects, type of crystal, spatial variability

Shield	Sig RMSE, mm (%)	Sig Bias, mm (%)	Exp RMSE, mm (%)	Exp Bias, mm (%)
US UN	0.18 (16.8)	0.00 (0.4)	0.19 (17.5)	0.00 (0.6)
All SA	0.24 (22.9)	−0.02 (−1.8)	0.25 (24.4)	−0.02 (−2.0)
NOR SA	0.46 (37.3)	−0.06 (−4.5)	0.46 (36.7)	−0.02 (−1.3)
US SA	0.13 (14.0)	−0.01 (−0.6)	0.14 (15.2)	−0.00 (−0.5)
US DA	0.13 (13.9)	0.00 (0.0)	0.14 (13.8)	0.00 (0.1)
US BDA	0.12 (13.6)	−0.01 (−1.7)	0.13 (14.6)	−0.00 (−0.9)
US SDFIR	0.13 (14.1)	−0.01 (−0.09)	0.13 (14.2)	−0.01 (−1.6)

sDFIR and DFIR respond similarly to wind speed

Measurement noise and spatial variability of precipitation

Results:

Exponential Transfer Function

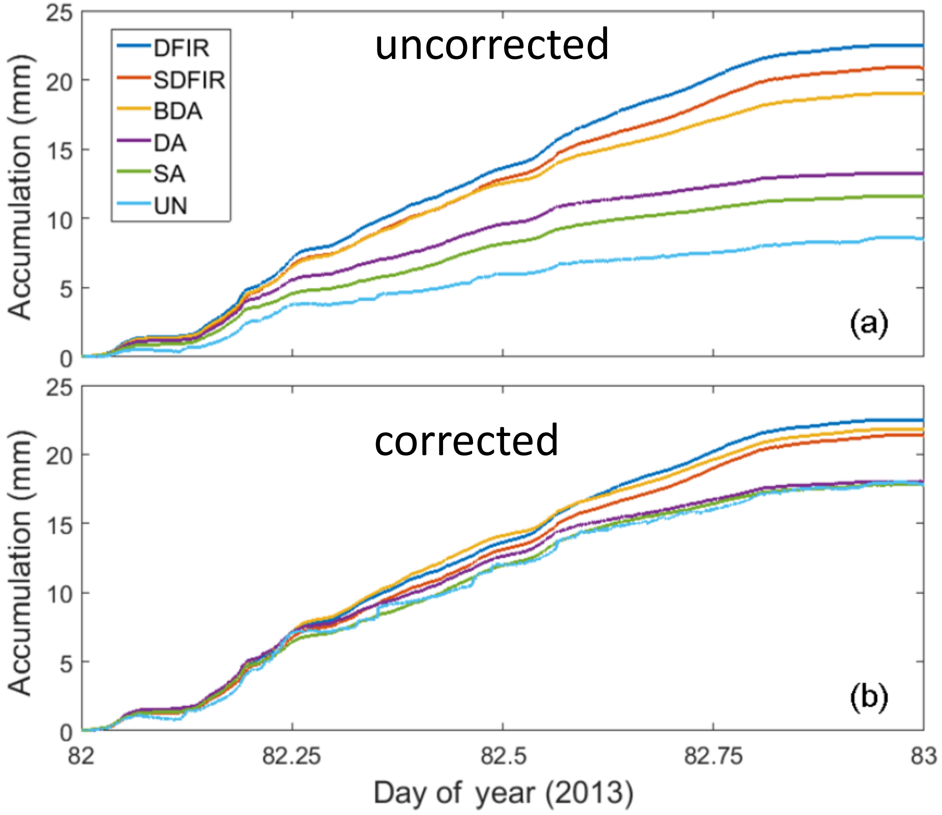

T_{mean}=-6-6°C, W_{mean}=3.6m/s

SNOW ONLY T<-2.5°C

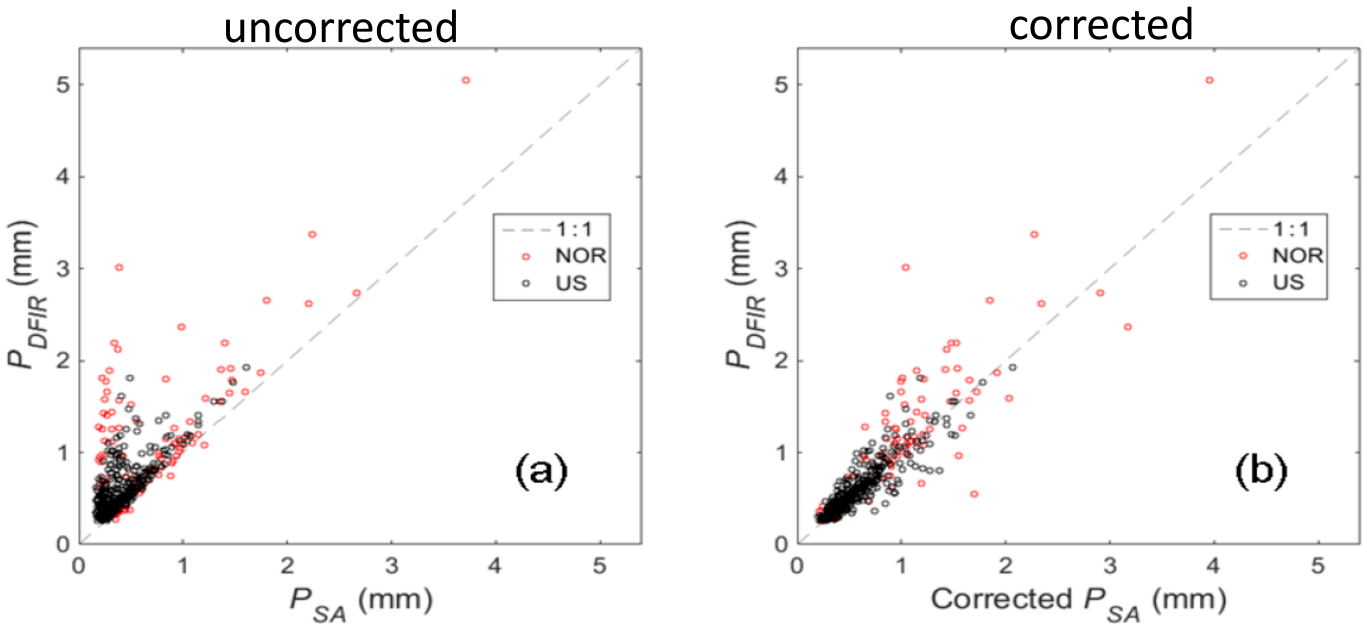

Still some dispersion persists, which may indicate that not all influencing variables have been investigated yet.

Exponential transfer Function, *Kochendorfer et al. (2017b)*

- Data from SPICE project
- eight sites
- Temperature measurements
- Wind measurements a 10m and gauges height

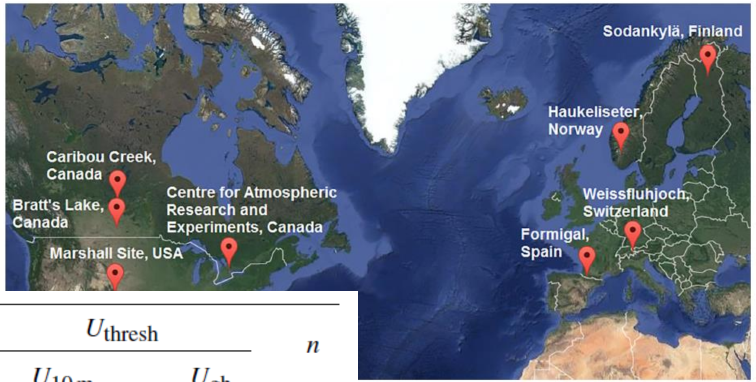

$$\boxed{\mathrm{CE} = e^{-a(U)\left(1-\left[\tan^{-1}(b(T_{\mathrm{air}}))+c\right]\right)}}$$

Shield	$f(U_{\mathrm{gh}}, T_{\mathrm{air}})$			$f(U_{10\,\mathrm{m}}, T_{\mathrm{air}})$			U_{thresh}		n
	a	b	c	a	b	c	$U_{10\,\mathrm{m}}$	U_{gh}	
UN	0.0785	0.729	0.407	0.0623	0.776	0.431	$9\,\mathrm{m\,s^{-1}}$	$7.2\,\mathrm{m\,s^{-1}}$	3774
SA	0.0348	1.366	0.779	0.0281	1.628	0.837	$9\,\mathrm{m\,s^{-1}}$	$7.2\,\mathrm{m\,s^{-1}}$	3725

Without explicitly including Temperature

~~T≥2°C rain~~

-2<T<2 °C mixed

T≤-2 °C snow

$$\boxed{\mathrm{CE} = (a)e^{-b(U)} + c}$$

Shield	Phase	$f(U_{\mathrm{gh}})$			$f(U_{10\,\mathrm{m}})$			U_{thresh}		n
		a	b	c	a	b	c	$U_{10\,\mathrm{m}}$	U_{gh}	
UN	mixed	0.641	0.236	0.356	0.624	0.185	0.364	$9\,\mathrm{m\,s^{-1}}$	$7.2\,\mathrm{m\,s^{-1}}$	1245
UN	solid	0.860	0.371	0.229	0.865	0.298	0.225	$9\,\mathrm{m\,s^{-1}}$	$7.2\,\mathrm{m\,s^{-1}}$	1968
SA	mixed	0.668	0.132	0.339	0.821	0.077	0.175	$9\,\mathrm{m\,s^{-1}}$	$7.2\,\mathrm{m\,s^{-1}}$	1297
SA	solid	0.728	0.230	0.336	0.742	0.181	0.322	$9\,\mathrm{m\,s^{-1}}$	$7.2\,\mathrm{m\,s^{-1}}$	1929

Pre-SPICE: *Kochendorfer et al. (2017a)*

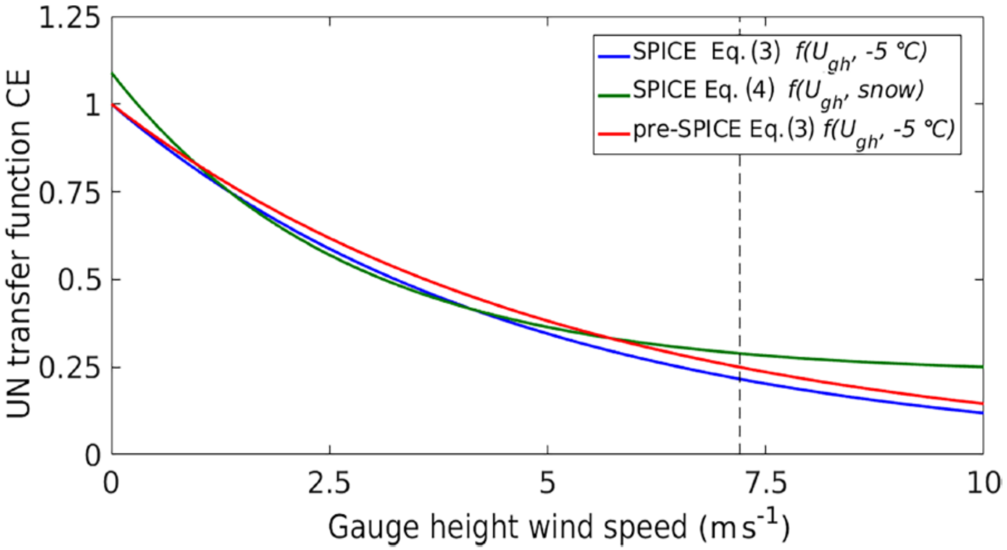

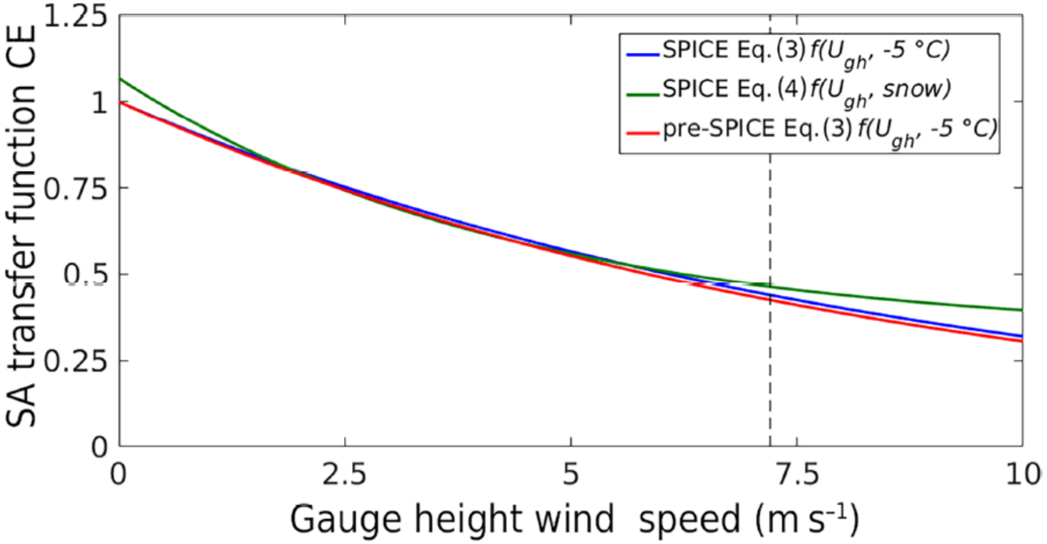

Results:

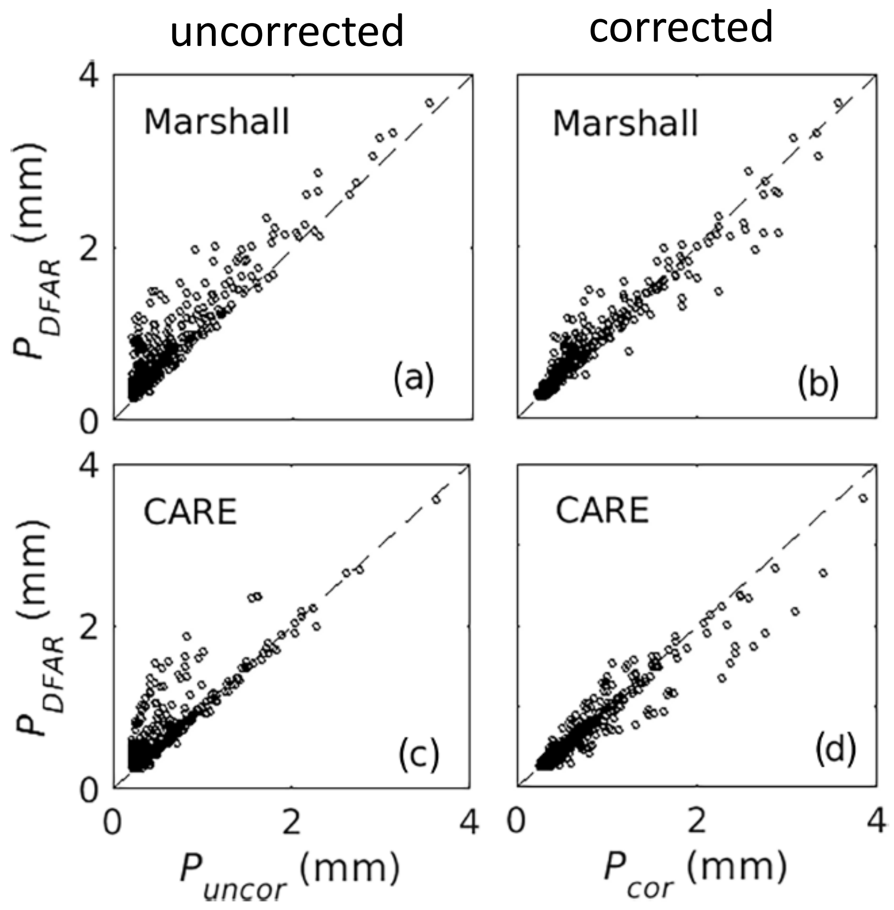

Error statistics:

The associated RMSE, bias, correlation coefficient (r), and the percentage of events within 0.1mm ($PE_{0.1mm}$) were estimated for all eight sites.

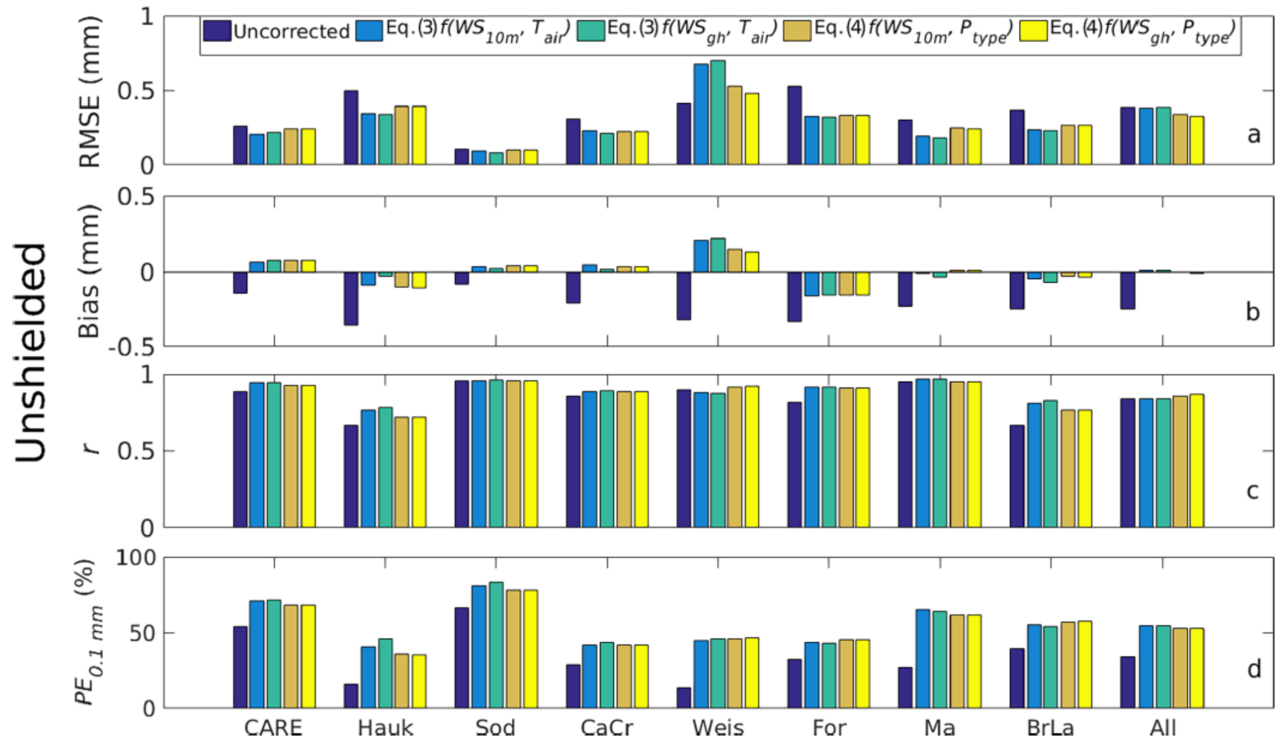

Residual errors are ascribed to the random spatial variability of precipitation, the crystal variability, the different principles of measure and the measurement noise.

Still some dispersion persists, which may indicate that not all influencing variables have been investigated yet.

Transfer Function in the Spanish operational network, *Buisán S.T: et al. (2017)*

- Data from SPICE project, winter 2014-2015
- Site: Formigal-Sarrios (Pyrenees)
- Wind measurements at 10 m height with a heated anemometer
- Gauges orifice height = 3.5 m

Objectives:

- Assessment of snowfall accumulation
- Assessment of Tipping Bucket Thies (TPB) rain gauge performance because is the gauge widely used by Spanish Meteorological State Agency (AEMET)

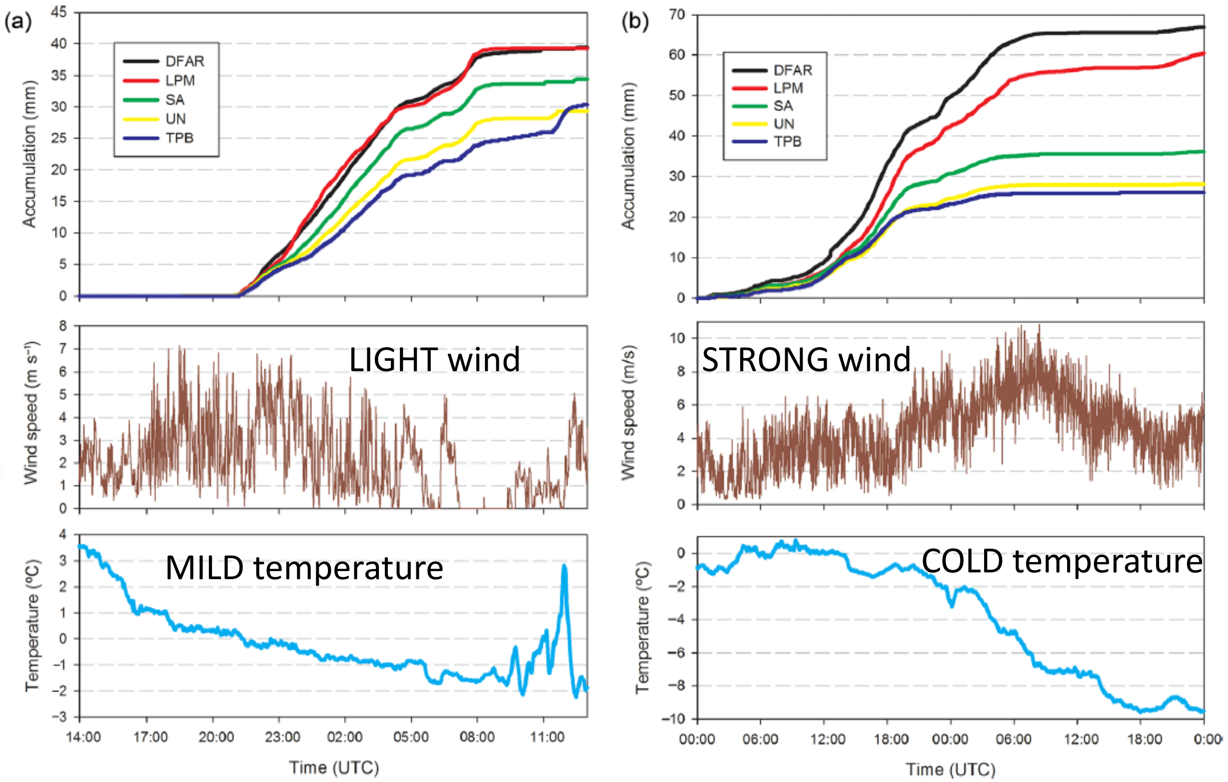

Instrument (Manufacturer)	Configuration
Weighing gauge Pluvio^2 (OTT)	DFIR
Disdrometer LaserPM (Thies)	DFIR
Weighing gauge Pluvio^2 (OTT)	Single Alter
Weighing gauge Pluvio^2 (OTT)	Unshielded
Tipping bucket (Thies)	Unshielded

Accumulation period:

1h → 214 data

- 114 events to calculate the regression equation
- 100 to test it

3h→ 87 data

- 45 events to calculate the regression equation
- 42 to test it

1 h transfer functions	
$CR = 0.87 \times \exp(-0.198 \times W)$	$R^2 = 0.49$
$CR = 1.01 \times \exp(0.077 \times T - 0.176W)$	$R^2 = 0.57$
$CR = 0.925 \times \exp(0.069 \times T - 0.176 \times W + 0.078 \times \text{Acc})$	$R^2 = 0.60$
True accumulation (1 h) = Acc/CR – 0.095 × Acc/CR + 0.095 × Acc (previous hour)	
3 h transfer functions	
$CR = 0.84 \times \exp(-0.234 \times W)$	$R^2 = 0.52$
$CR = 1.04 \times \exp(0.094 \times T - 0.201W)$	$R^2 = 0.60$
$CR = 0.892 \times \exp(0.067 \times T - 0.212 \times W + 0.049 \times \text{Acc})$	$R^2 = 0.65$
True accumulation (3 h) = Acc/CR	

Melt delay

No melt delay

1h accumulation

(a)

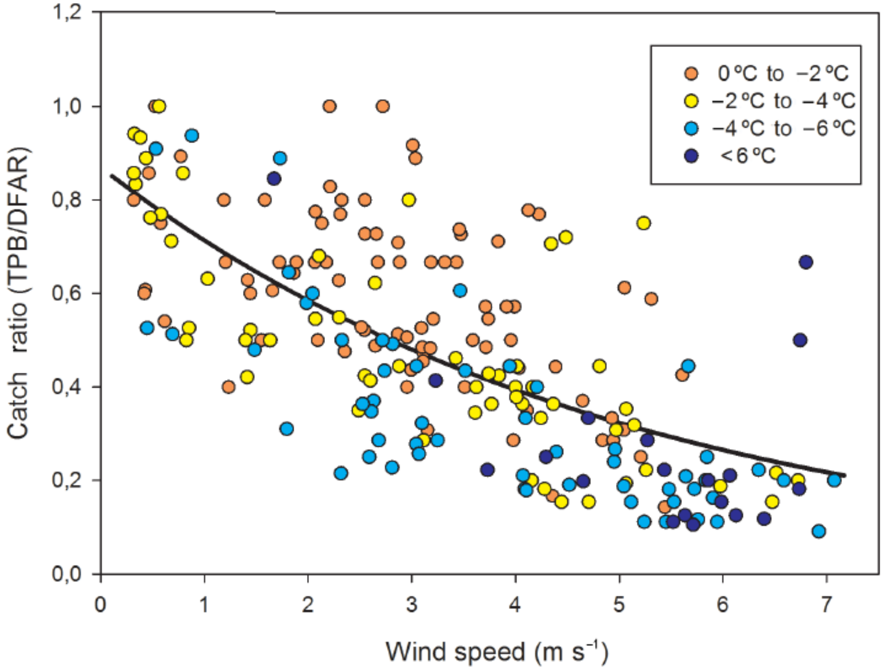

3h accumulation

(b)

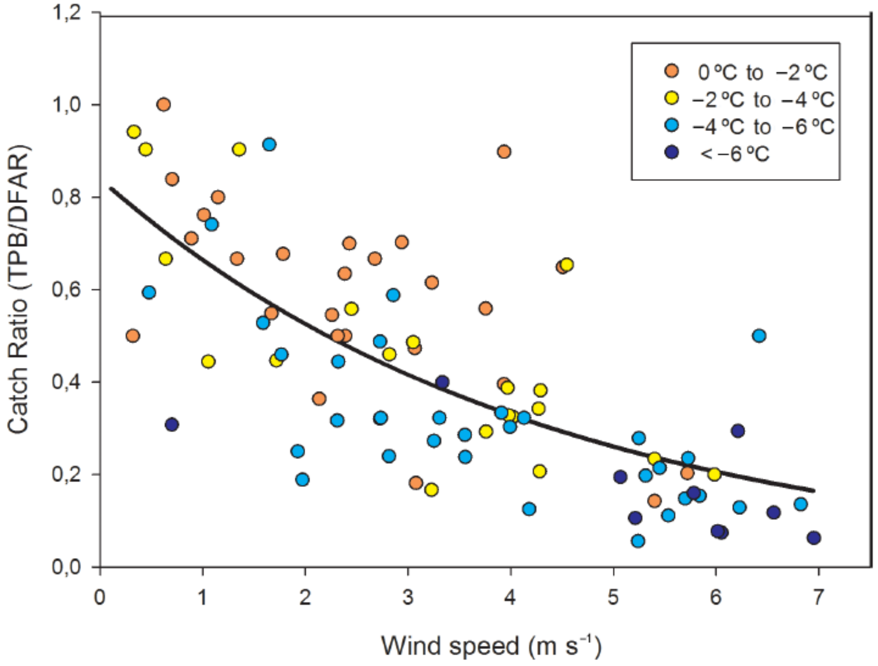

References

- Wolff, M. A., Isaksen, K., Petersen-Øverleir, A., Ødemark, K., Reitan,T., and Brækkan, R.: *Derivation of a new continuous adjustment function for correcting wind-induced loss of solid precipitation: results of a Norwegian field study*, Hydrol. Earth Syst. Sci., 19, 951–967, 2015.
- Førland, E. J., Allerup, P., Dahlström, B., Elomaa, E., Jónsson, T., Madsen, H., Perälä, J., Rissanen, P., Vedin, H., and Vejen, F.: *Manual for operational correction of Nordic precipitation data*, DNMI report Nr. 24/96, Norwegian Meteorological Institute, Oslo, Norway,1996.
- Kochendorfer, J., Rasmussen, R., Wolff, M., Baker, B., Hall, M. E., Meyers, T., Landolt, S., Jachcik, A., Isaksen, K., Brækkan, R., and Leeper, R.: *The quantification and correction of wind induced precipitation measurement errors,* Hydrol. Earth Syst.Sci., 21, 1973–1989, 2017a.
- John Kochendorfer, Rodica Nitu, MareileWolff, Eva Mekis, Roy Rasmussen, Bruce Baker, Michael E. Earle, Audrey Reverdin, KaiWong, Craig D. Smith, Daqing Yang, Yves-Alain Roulet, Samuel Buisan, Timo Laine, Gyuwon Lee, Jose Luis C. Aceituno, Javier Alastrué, Ketil Isaksen, Tilden Meyers, Ragnar Brækkan, Scott Landolt, Al Jachcik, and Antti Poikonen: *Analysis of single-Alter-shielded and unshielded measurements of mixed and solid precipitation from WMO-SPICE,* Hydrol. Earth Syst.Sci., 21, 3525–3542, 2017b.
- Samuel T. Buisán, Michael E. Earle, José Luís Collado, John Kochendorfer, Javier Alastrué, MareileWolff, Craig D. Smith, and Juan I. López-Moreno: *Assessment of snowfall accumulation underestimation by tipping bucket gauges in the Spanish operational network,* Atmos. Meas. Tech., 10, 1079–1091, 2017.
- Thériault J.M., Rasmussen R., Petro E., Trépanier J.Y., Colli M. and Lanza L.G.: *Impact of Wind Direction, Wind Speed, and Particle Characteristics on the Collection Efficiency of the Double Fence Intercomparison Reference,* Journal of Applied Meteorology and Climatology, 54, 1918-1930,2015.

Section 2

CFD simulations:
STATE OF THE ART

Navier-Stokes equations

Hp:
Newtonian fluid
Incompressible

$$\boldsymbol{T} = -p\boldsymbol{I} + 2\mu\boldsymbol{D}$$

T is the *stress tensor*
D is the *deformation rate tensor*

The equations of motion

$$\frac{\partial u_\alpha}{\partial t} + \boldsymbol{u}\cdot\boldsymbol{\nabla}u_\alpha = -\frac{1}{\rho}\frac{\partial p}{\partial x_\alpha} + g_\alpha + \upsilon\partial^2 u_\alpha$$

$$\boldsymbol{\nabla}\cdot\boldsymbol{u} = 0$$

Reynolds Average Navier-Stokes equations (RANS):

$u_i(\mathbf{x},t)=\overline{u_i}(\mathbf{x},t)+u_i'(\mathbf{x},t)$

$p(\mathbf{x},t)=\bar{p}(\mathbf{x},t)+p'(\mathbf{x},t)$

$\overline{u_i}$ and $\bar{p}$ are the mean of flow velocity components and pressure

u_i' and p' are the fluctuations

$$\frac{\partial\overline{u_i}}{\partial t} + \overline{u_j}\frac{\partial\overline{u_i}}{\partial x_j} = -\frac{1}{\rho}\frac{\partial\bar{p}}{\partial x_i} + \upsilon\frac{\partial^2\overline{u_i}}{\partial x_j\partial x_j} - \frac{\partial\overline{(u_j'u_i')}}{\partial x_j}$$

$$\frac{\partial\overline{u_i}}{\partial x_i} = 0$$

Large Eddies simulation (LES):

G is Filter function $\quad \bar{u}_\alpha(\boldsymbol{x},t) = \iiint_{-\infty}^{+\infty} G_\Delta(\boldsymbol{x}-\boldsymbol{y})u_\alpha(\boldsymbol{x},t)d^3x$

$$\frac{\partial\overline{u_\alpha}}{\partial t} + \overline{\boldsymbol{u}}\cdot\frac{\partial\overline{u_\alpha}}{\partial x_j} = -\frac{1}{\rho}\frac{\partial\bar{p}}{\partial x_\alpha} + \upsilon\frac{\partial^2\overline{u_\alpha}}{\partial x_j\partial x_j} - \frac{\partial\tau_{\alpha j}}{\partial x_j}$$

$$\frac{\partial\overline{u_\alpha}}{\partial x_\alpha} = 0$$

$\overline{u_\alpha}$ are the components of the filtered field

Subgrid scales are modelled through the stress tensor ($\tau_{\alpha j}$)

e.g.
k-ε, k-ω and SST k-ω ← Closure problem→ models → e.g.
Smagorinsky

Advantages:
- Lover computational cost compared to LES simulation
- Good description of the mean flow velocities features

Disadvantage:
-The URANS fails to account for the unsteady turbulent fluctuations

Advantage:
- Calculation of the unsteady turbulent fluctuation until the detached scale

Disadvantage:
- High computational cost

State of the art: Lagrangian Tracking Model

Colli M., PhD thesis:
Assessing the accuracy of precipitation gauges: a CFD approach to model wind induced errors
Supervisor: Prof. Ing. Luca G. Lanza,
External Referee: Dr. Roy Rasmussen

SOLID PRECIPITATION PARTICLES (wet / dry)

Shielded and unshielded gauges

Uncoupled approach for particle trajectories

Eulerian model

Computational Fluid Dynamics Simulations (CFD) :
- RANS (SST k-omega)
- LES

Result: Air velocity ($\mathbf{v}_a$)

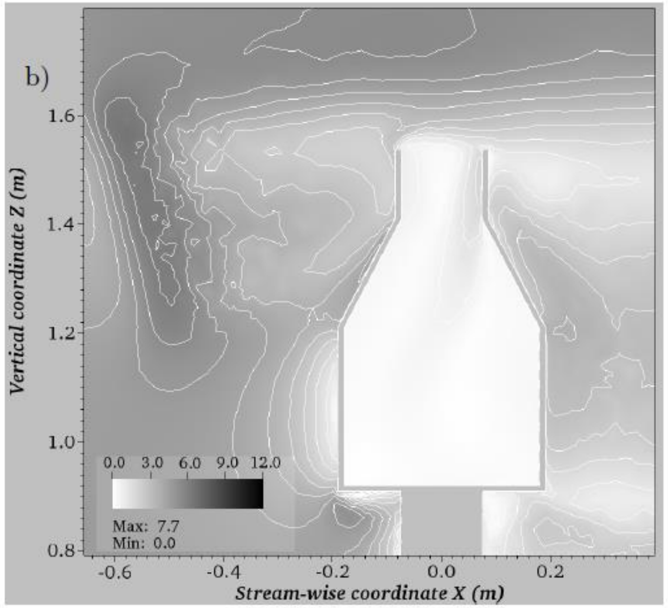

RANS simulation: Magnitude of velocity Uw=5m/s

Lagrangian particle tracking model
Equation of motion

$$V_p \rho_p \mathbf{a_p} = -C_D A_p \rho_a 0.5(\mathbf{v_p} - \mathbf{v_a})|\mathbf{v_p} - \mathbf{v_a}| + V_p(\rho_p - \rho_a)\mathbf{g}$$

Simplification : use of a <u>fixed CD,</u> function of particles terminal velocity w_T

$$Re_p = \frac{D w_t}{\upsilon_a}$$

CE calculated from the simulation model: $CE_{vol} = \frac{\sum_0^D \rho_p V * n(d) * N(d)}{\sum_0^D \rho_p V * n_{max}(d) * N(d)}$

State of the art: improvements

“**An Improved Trajectory Model to Evaluate the Collection Performance of Snow Gauges**”, Colli et al. 2015.

The drag coefficient was estimated using the local Reynolds number as derived from CFD simulations

$$Re_p = \frac{D\,|V_p - V_a|}{\nu_a}$$

Validation by means of comparison of field data

$CD=f(Re_p)$

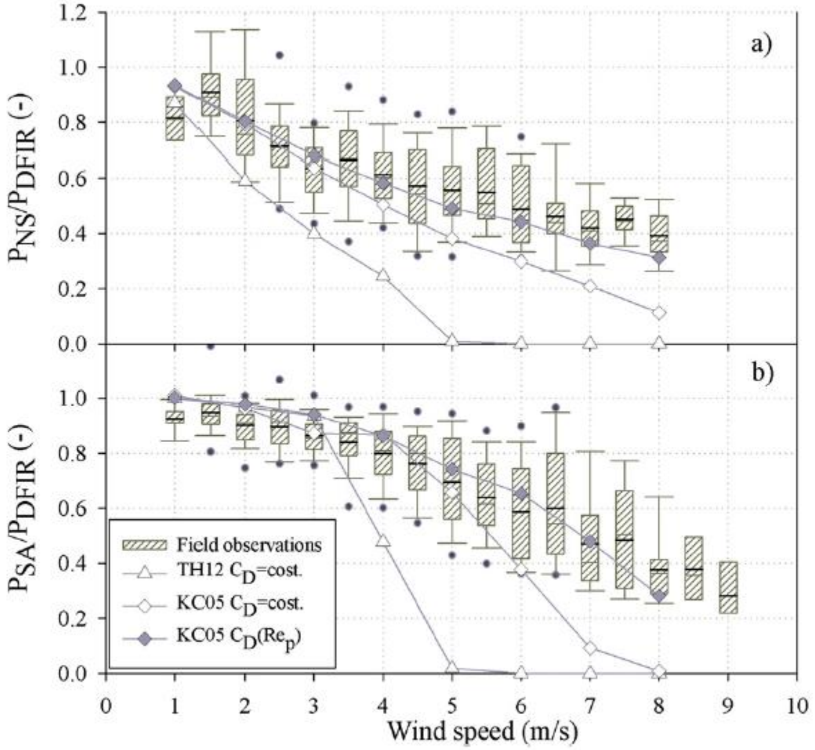

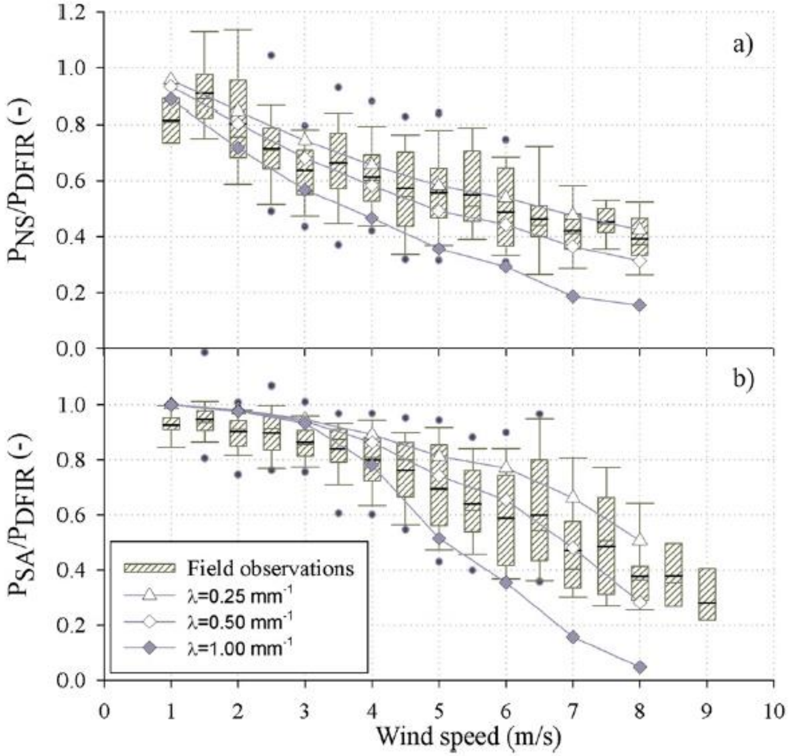

Type of precipitation: Drop Size Distribution DSD

Ulbrich (1983)

$$N(d) = N_0 d^k e^{-\Lambda d}$$

N0= scale parameter;
k= shape parameter;
Λ =slope parameter.

State of the art: LTM for the evaluation of the RAINFALL underestimation

"On the wind-induced undercatch in rainfall measurement using CFD-based simulations"
A. Cauteruccio, 2016.

RANS SST-k-omega CFD simulations

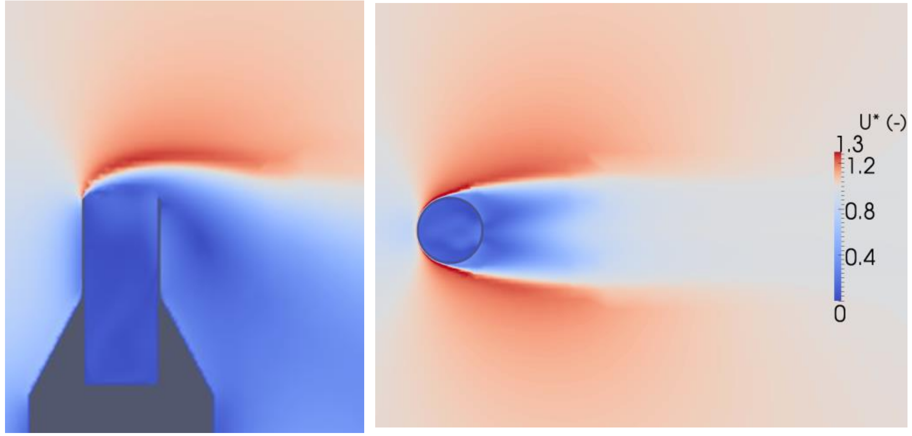

Normalized magnitude of velocity, Uw=5m/s

$Re=f(v_p-v_a)$

$C_D=f(Re_p)$

Lagrangian
Tracking model
LTM

From experimental data:

$\boxed{Re_p > 400}$

$$CD = y_0 + \frac{(ab)}{b + Rep}$$

with
a=3,4024
b=21,3834
y_0=0,4424

$\boxed{Re_p \leq 400}$

$$Re_p < 2 \qquad C_D = 1.06(24Re_p{}^{-1} + 2.400Re_p{}^{-0,045})$$
$$2 \leq Re_p < 21 \qquad C_D = 1.06(24Re_p{}^{-1} + 2.640Re_p{}^{-0,190})$$
$$21 < Re_p < 400 \qquad C_D = 1.06(24Re_p{}^{-1} + 4.536Re_p{}^{-0,368})$$

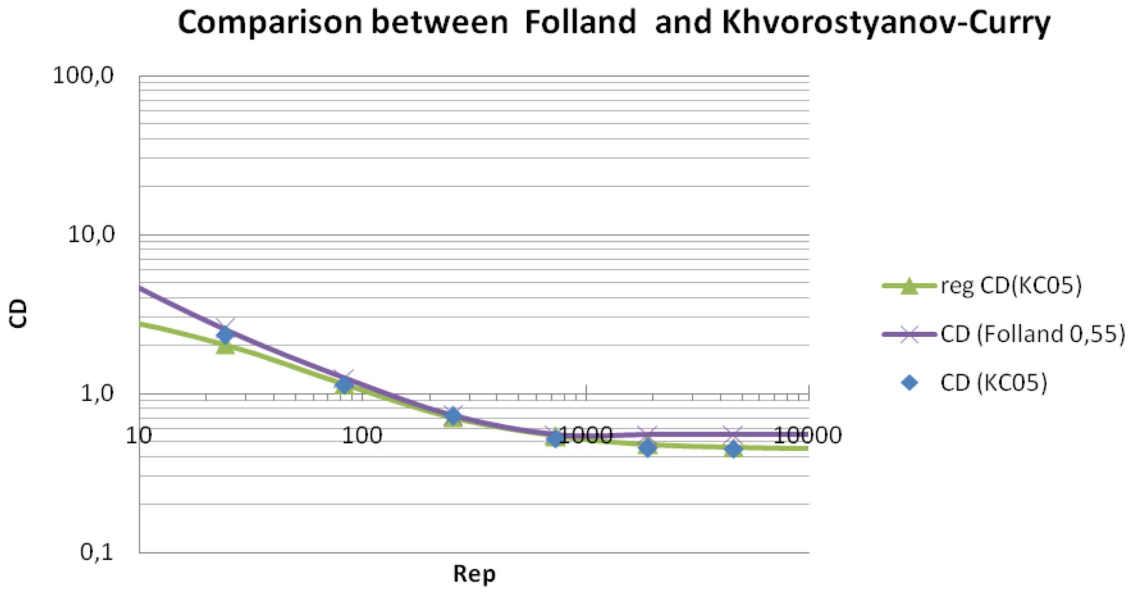

Some results

Ulbrich (1983)

$$N(d) = N_0 d^k e^{-\Lambda d}$$

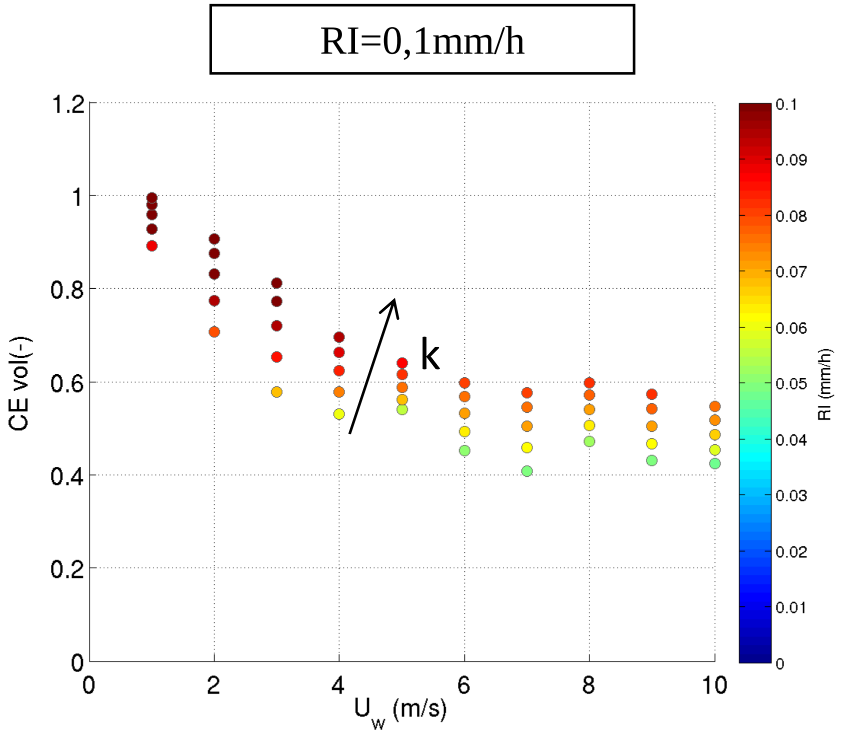

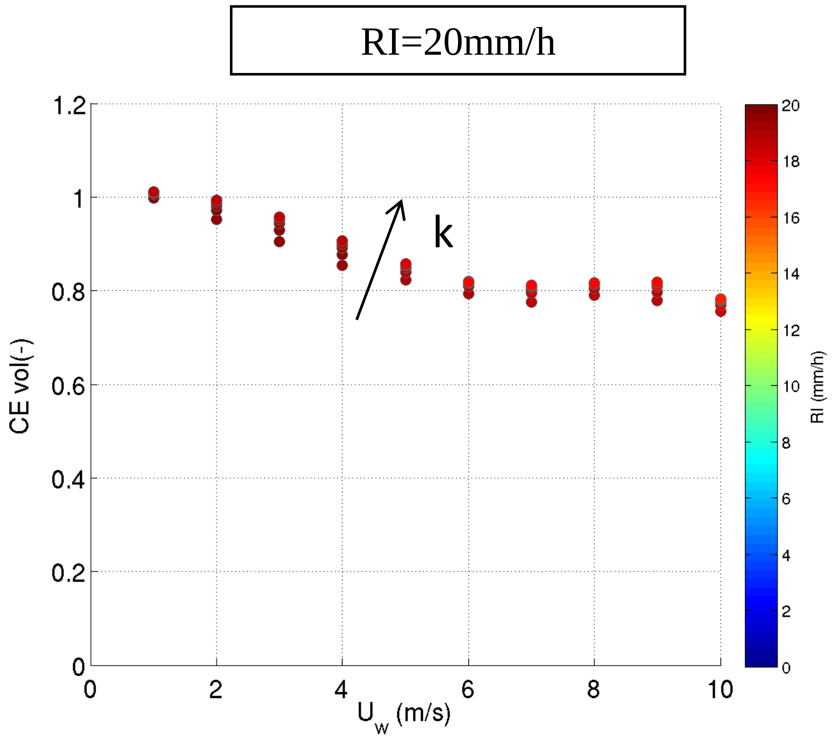

$$CE\ (U_w) = \frac{h_{mis}(U_w)}{h_r}$$

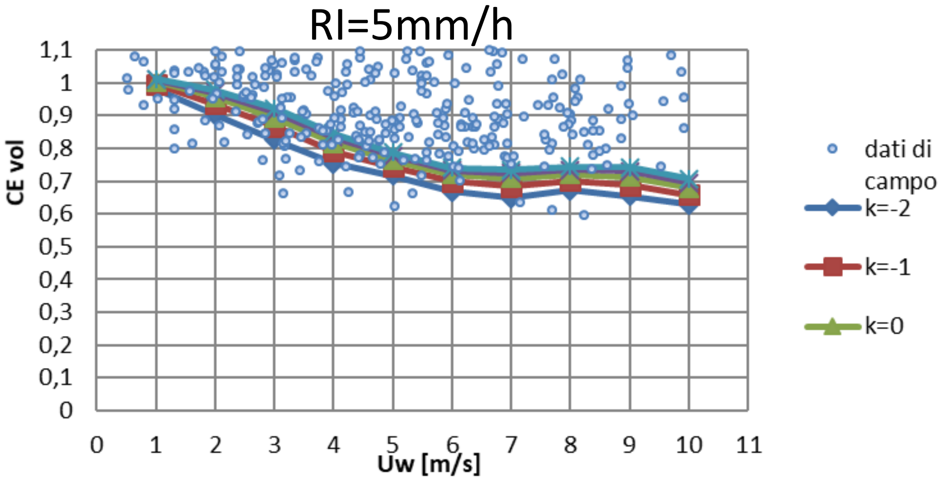

WMO DFIR

State of the art: the aerodynamic rain gauges

"**A Computational Fluid-Dynamics assessment of the improved performance of aerodynamic rain gauges**", Colli et al. 2018.

Traditional rain gauges with chimney and cylindrical shape

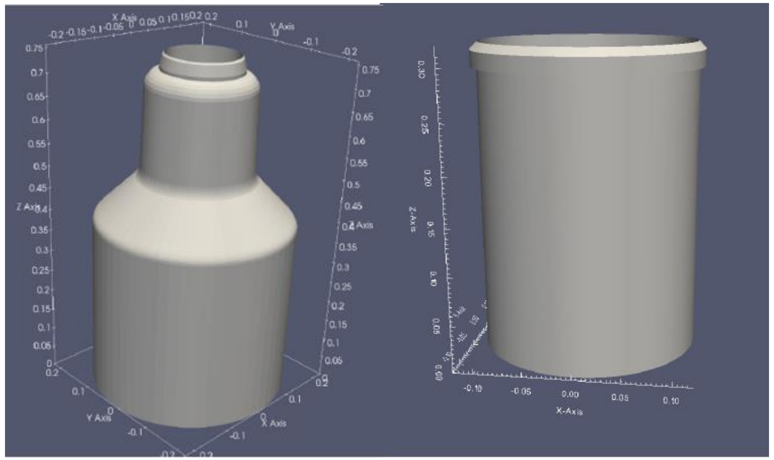

EML aerodynamics rain gauges with inverse conical shape

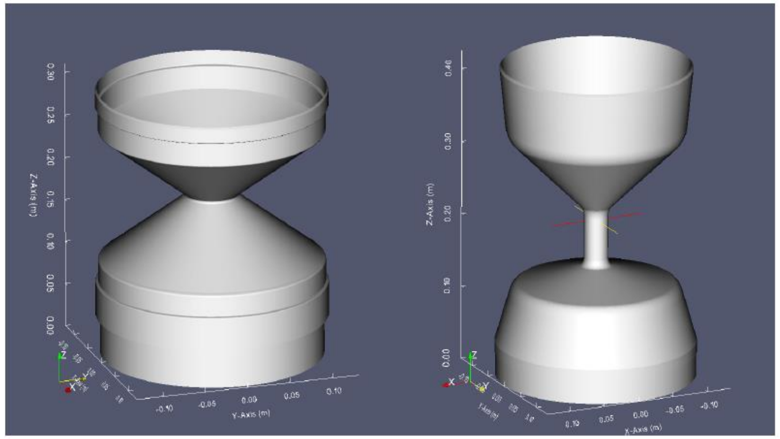

Aerodynamic rain gauges are developed to reduce the wind effects on precipitation measurement. These shapes are a possible alternative to the wind shields.

RANS SST k-omega simulations

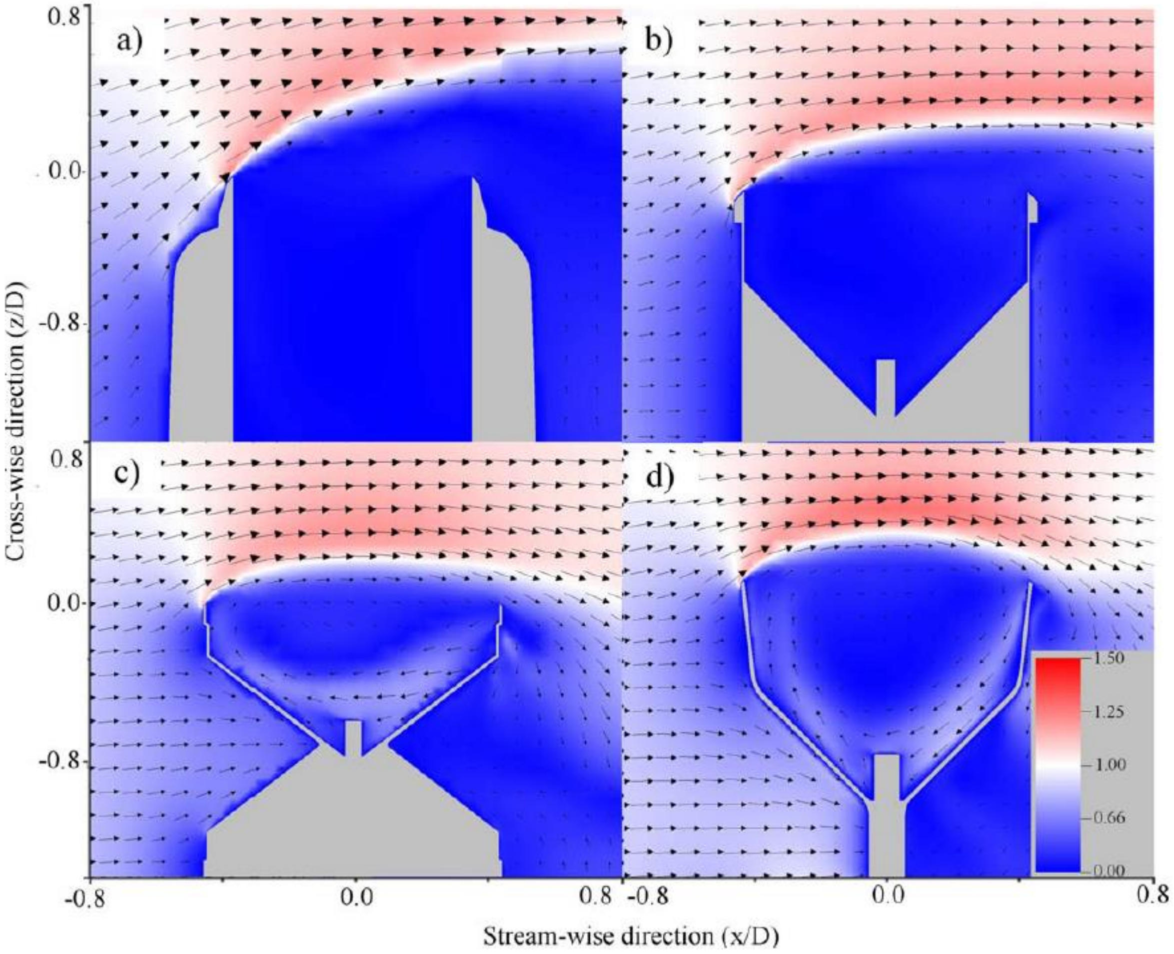

Non-dimensional magnitude of flow velocity. U_W=2m/s

RANS SST k-omega simulations

Non-dimensional vertical component of **air velocity** at the gauge collector level

U_w=2m/s

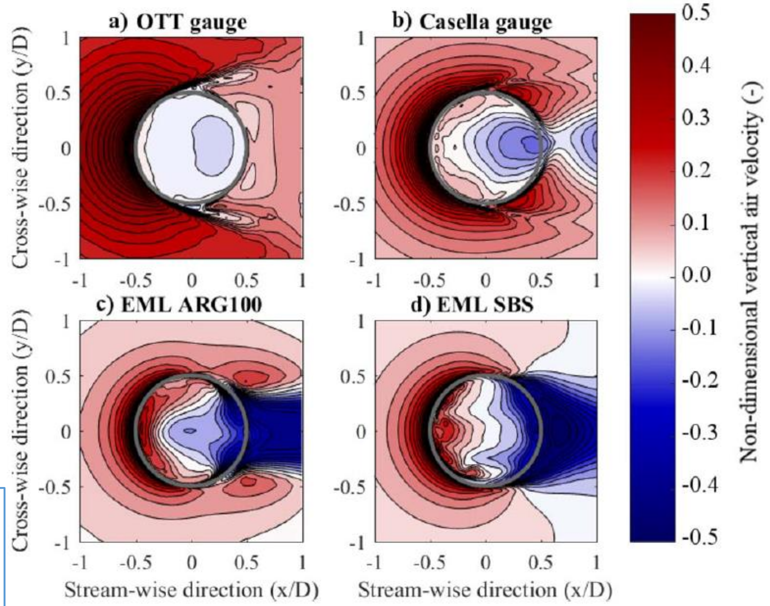

U_w=18m/s

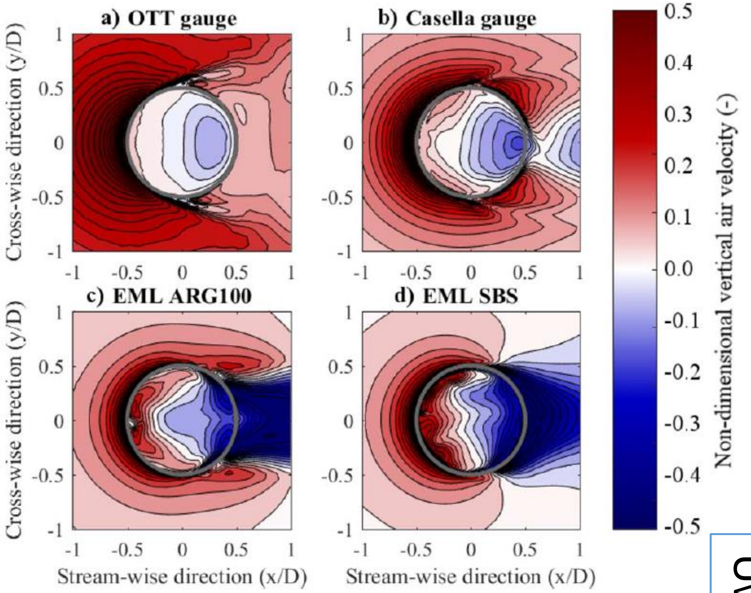

Non-dimensional airflow turbulent **kinetic energy** at the gauge collector level

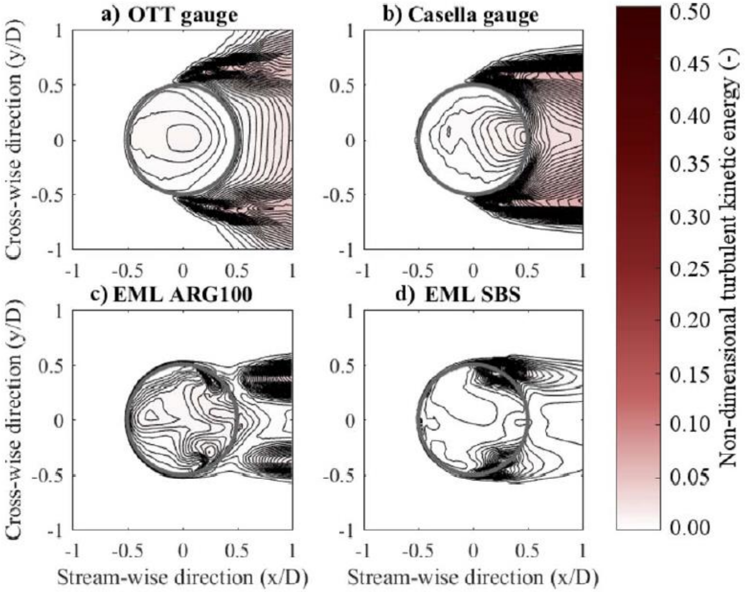

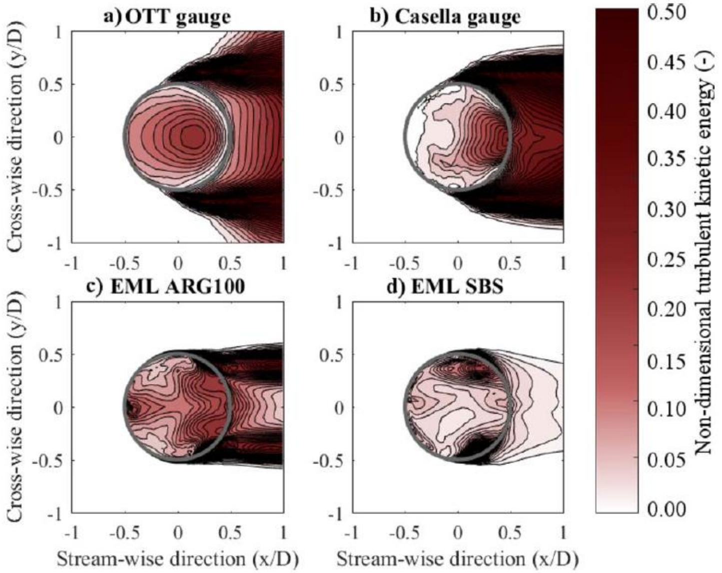

Non-dimensional horizontal component of the **airflow velocity** at the center of the collector

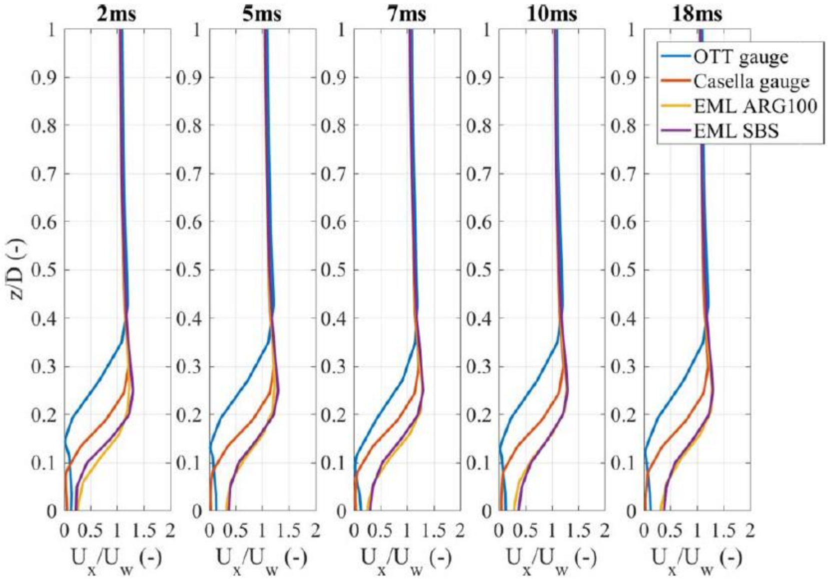

Non-dimensional airflow turbulent **kinetic energy** at the center of the collector

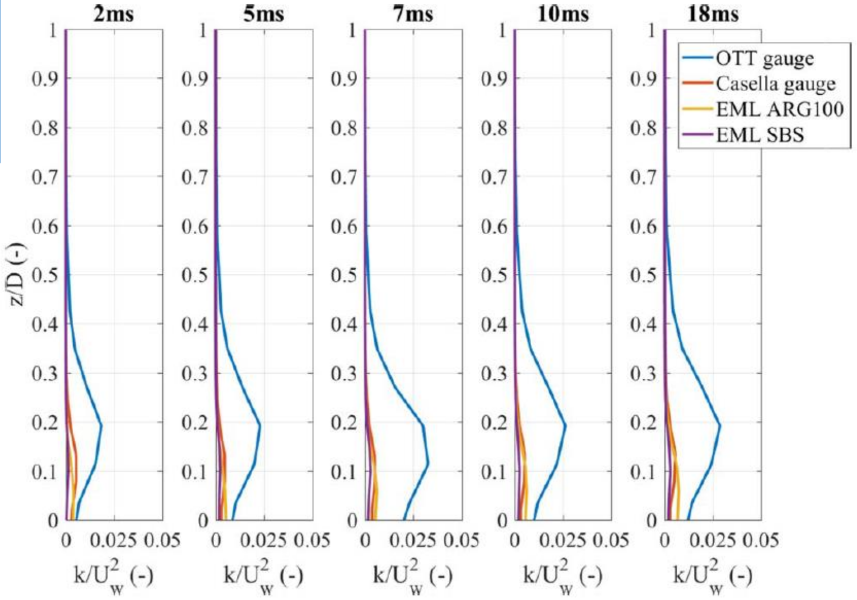

References

- Cauteruccio A., Colli M., Lanza L.G. *On the wind-induced undercatch in rainfall measurement using CFD-based simulations.* European Geosciences Union (EGU) General Assembly 2016, Vienna (Austria), 17-22 April 2016.
- Colli M., Lanza L.G., Rasmussen R., Thériault J.M., Baker B.C. and Kochendorfer J.: *an improved trajectory model to evaluate the collection performance of snow gauges.* J. of Applied Meteorology and Climatology, 54, 1826-1836, 2015.
- Colli M., Lanza L.G., Rasmussen R. and Thériault J.M. : *The collection efficiency of shielded and unshielded precipitation gauges. Part I: CFD airflow modeling.* J. of Hydrometeorology, 17, 231-243, 2016a.
- Colli M., Lanza L.G., Rasmussen R. and Thériault J.M.: *The collection efficiency of unshielded precipitation gauges. Part II: modeling particle trajectories.* J. of Hydrometeorology, 17, 245-255, 2016b.
- Colli M., Pollock M., Stagnaro M., Lanza L.G., Dutton M. and E. O’Connell: *A Computational Fluid-Dynamics assessment of the improved performance of aerodynamic rain gauges.* Water Resources Research, submitted (2018).

Section 3

Work in progress

CFD Simulations and WIND Tunnel measurements:

Comparison between different instrument shapes

Traditional rain gauges

Geonor T200B
weighing rain gauge

CAE PMB25 tipping
bucket rain gauge

Aerodynamic rain gauges

EML tipping bucket rain gauge

SBS500

Shielded snow gauge

Shield

Collector

Nipher gauge

DICCA/UNIGE Wind Tunnel facility

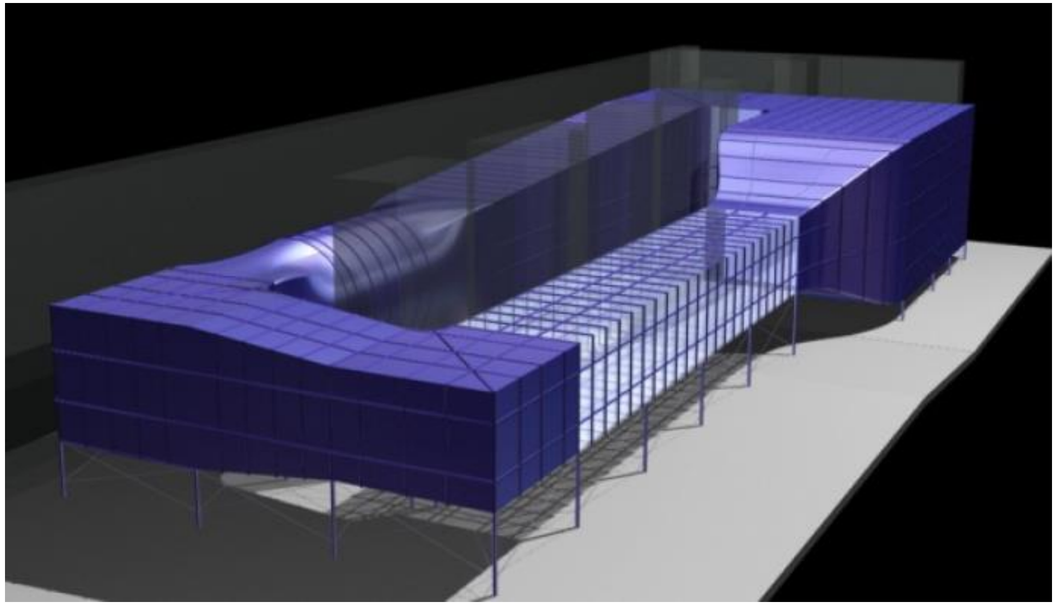

Dimension of the wind tunnel		Performance of the wind tunnel	
Width [m]	8	Design speed test chamber [m/s]	30
Length [m]	21	Maximum speed test chamber [m/s]	40
Height [m]	3.5	Power required to 40 m/s [kW]	100
Section test chamber [m^2]	1.7 x 1.35	Installed power [kW]	132
Length test chamber [m]	8.8	Power factor [-]	0.774
Ratio of contraction [-]	5		
Diameter fan [-]	2.2		

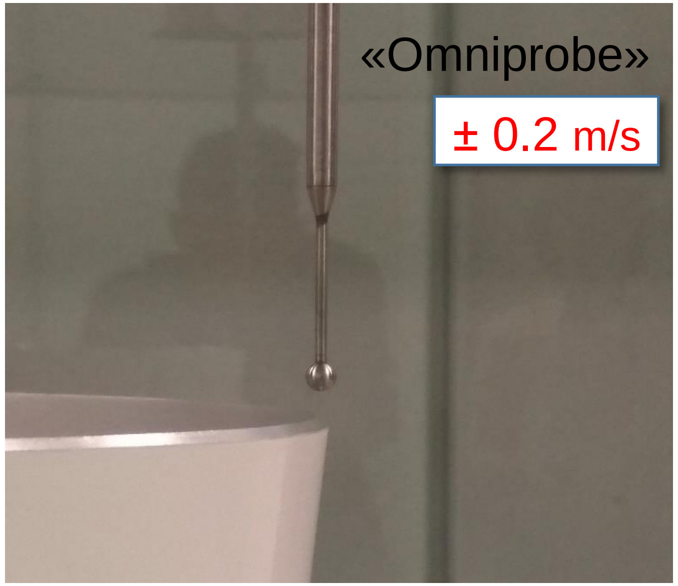

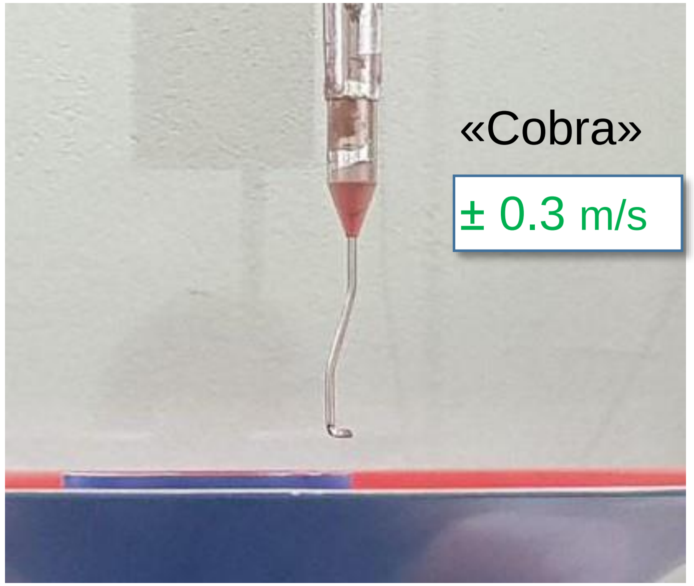

CFD framework:

Cae PMB25
5 x 6 x 4 m

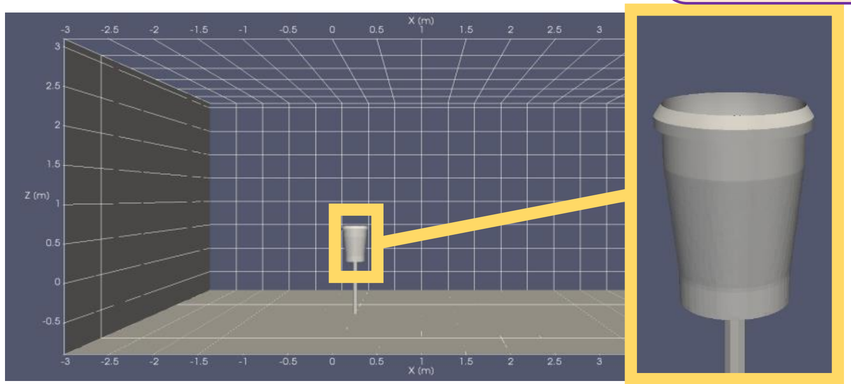

SBS500
5.8 x 5 x 2.2 m

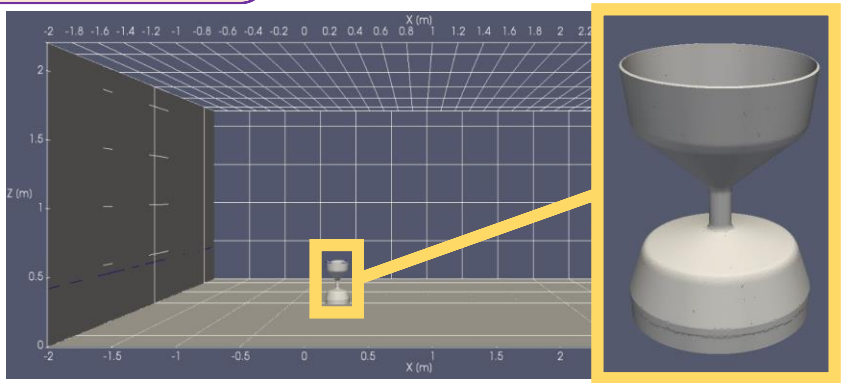

U

Geonor T200B
7 x 5 x 4 m

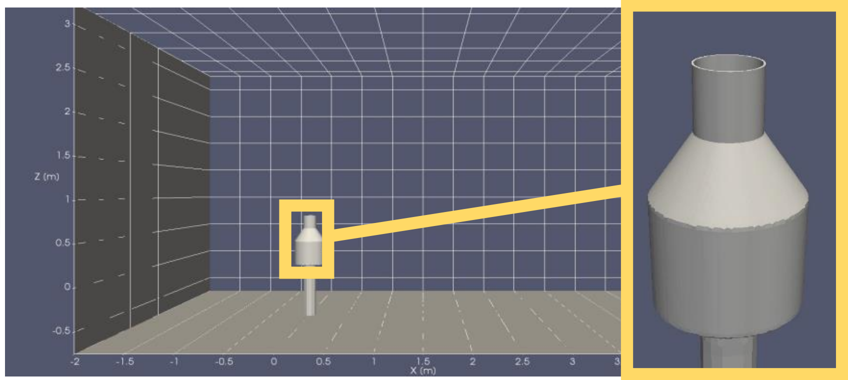

Nipher shielded
9 x 6 x 4.6 m

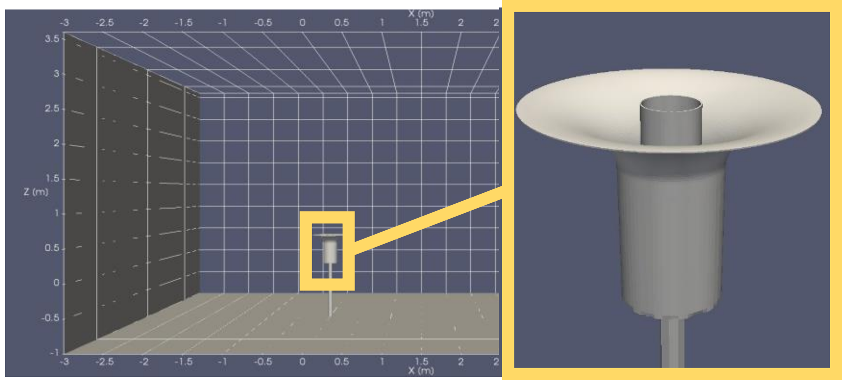

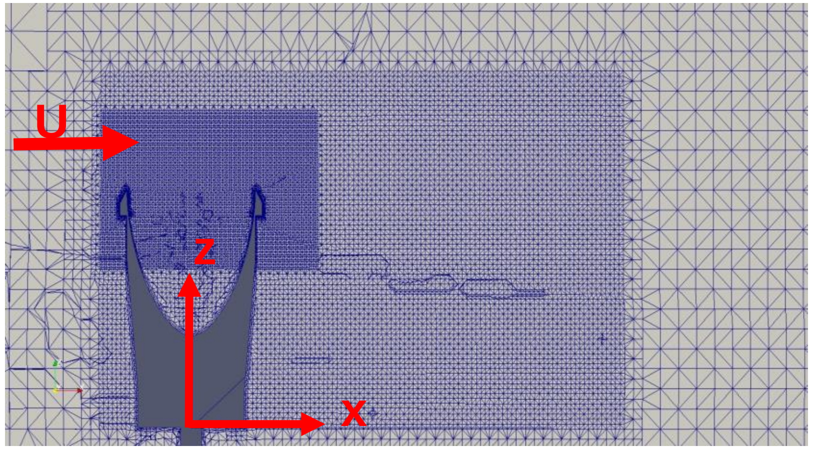

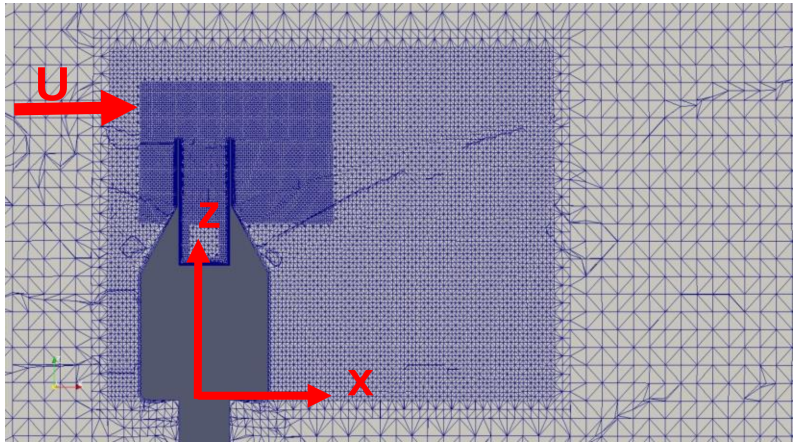

Some results

URANS SST k-omega simulations

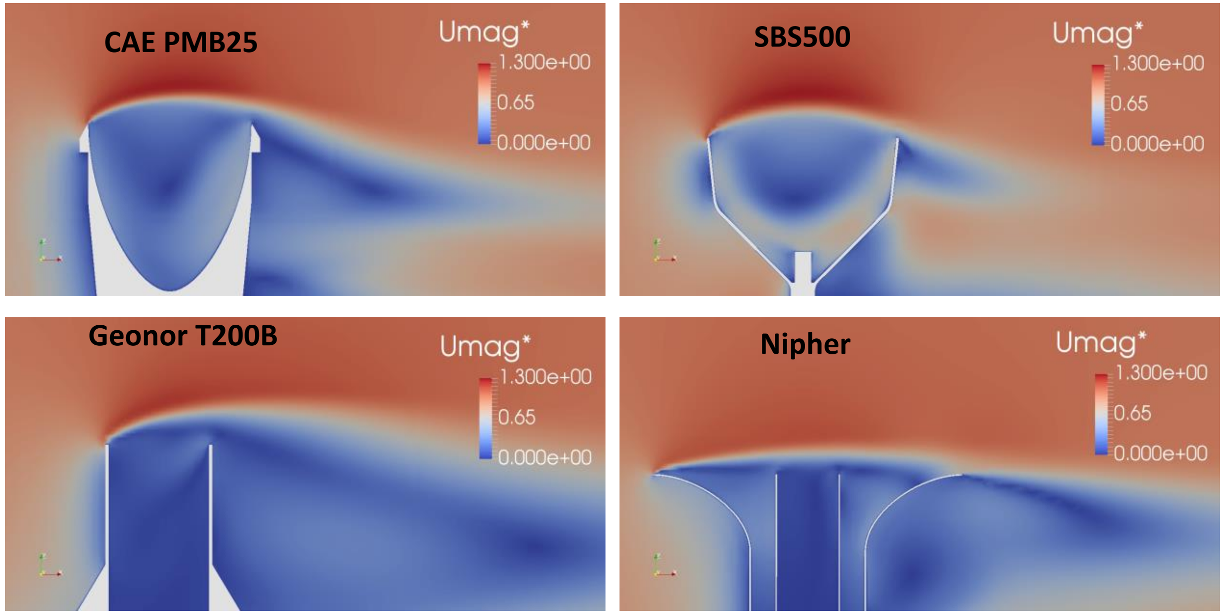

Normalized magnitude of flow velocity

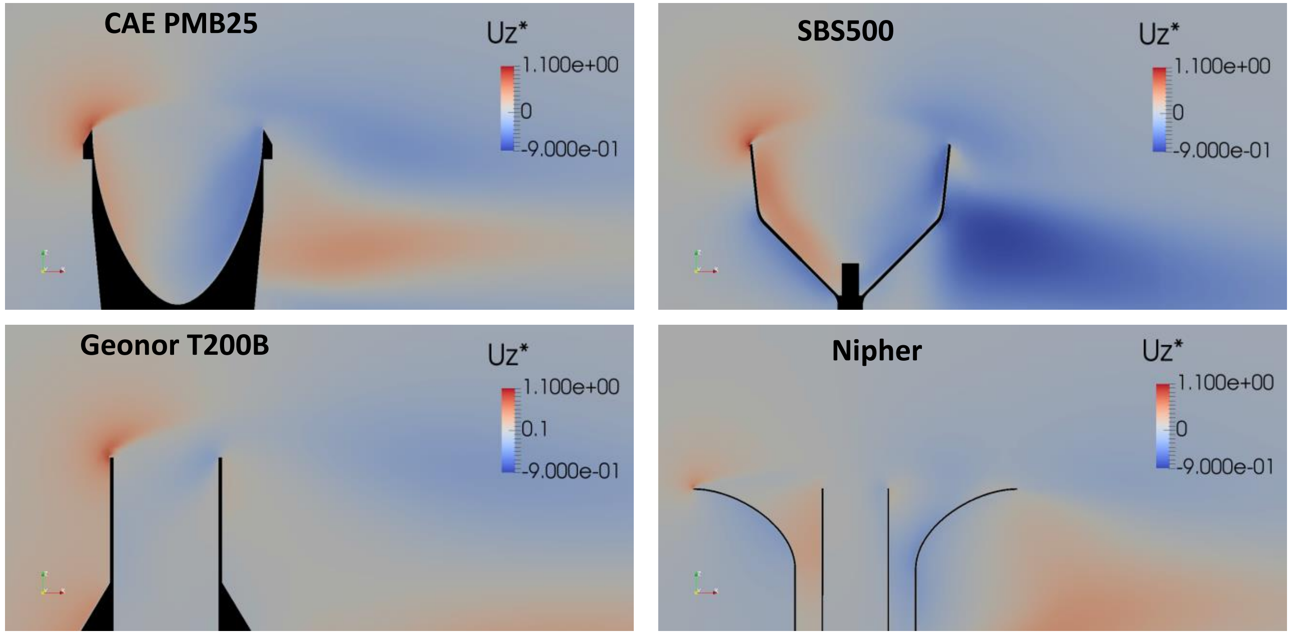

Normalized vertical component of flow velocity

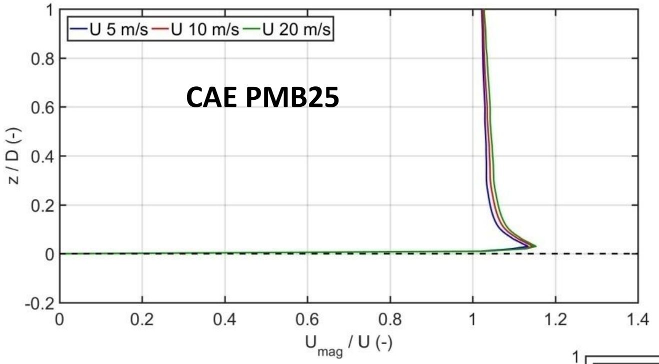

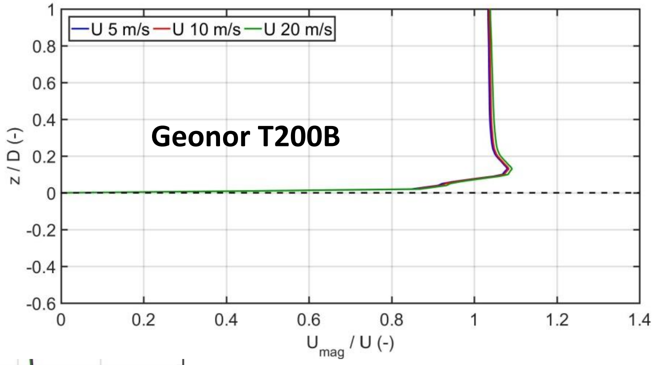

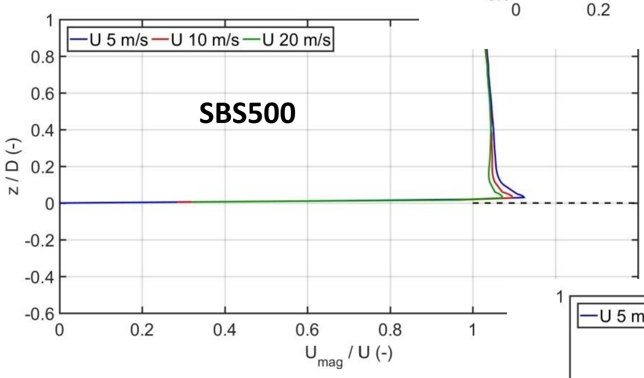

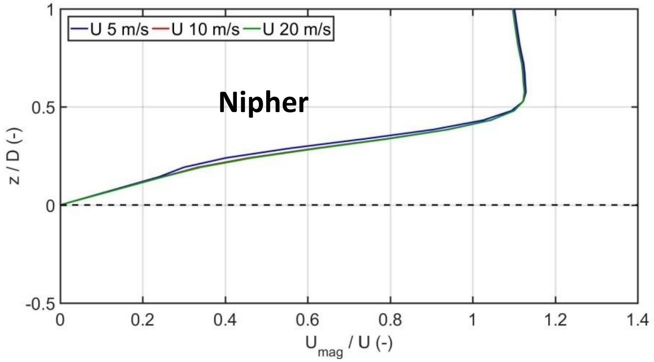

Normalize vertical profile of the magnitude at the centre of the orifice

The flow fields are scalable

Wind Tunnel validation

The SBS 500 tipping bucket

Vertical above the centre of the collector

U_W wind speed (inlet velocity) expressed in f: 10, 20,38 Hz

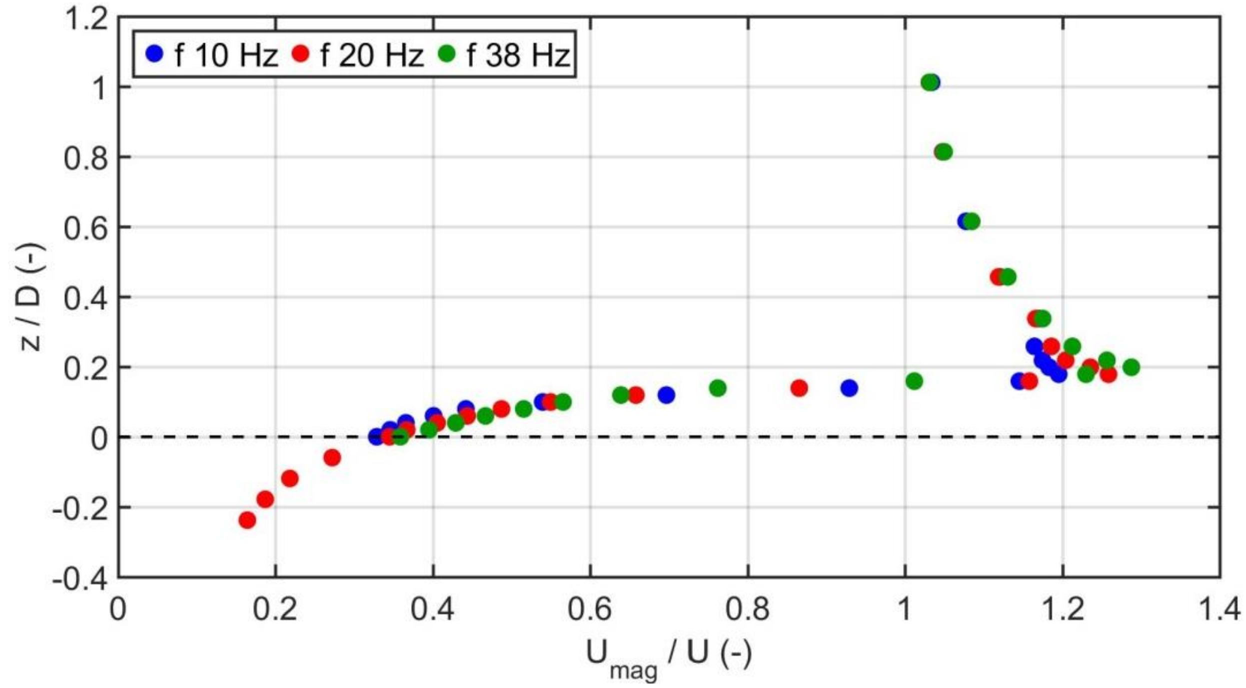

The scalability observed from CFD simulation is confirmed by WT measurements

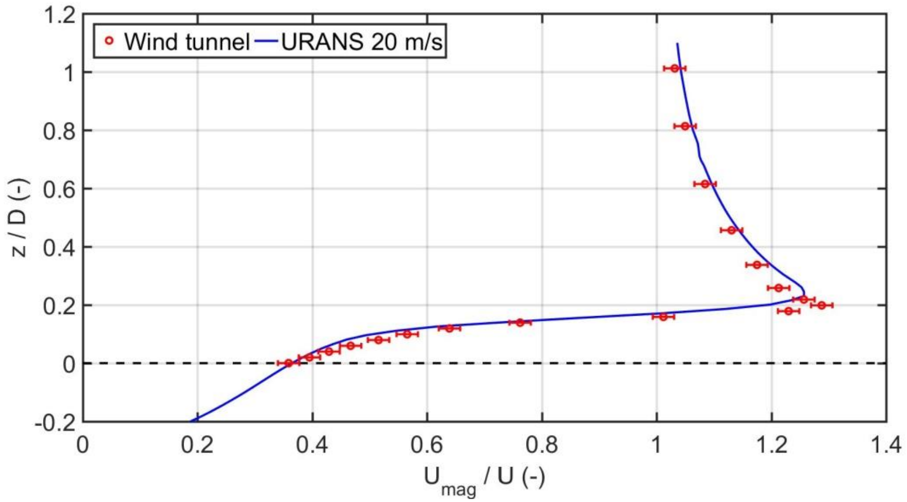

Good agreement between WT measurements and CFD results

Airflow around Kalyx rain gauge in uniform and turbulent base flows

Geometry

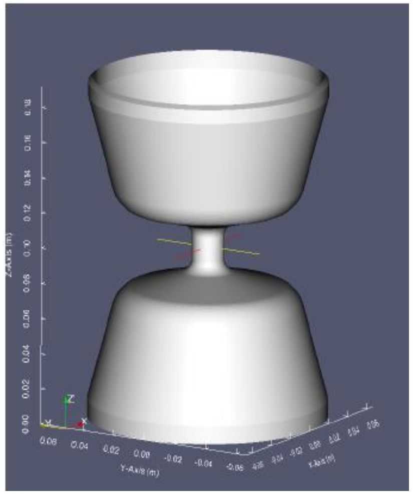

Kalix EML rain gauge

URANS SST k-omega simulations

1) Uniform base-flow

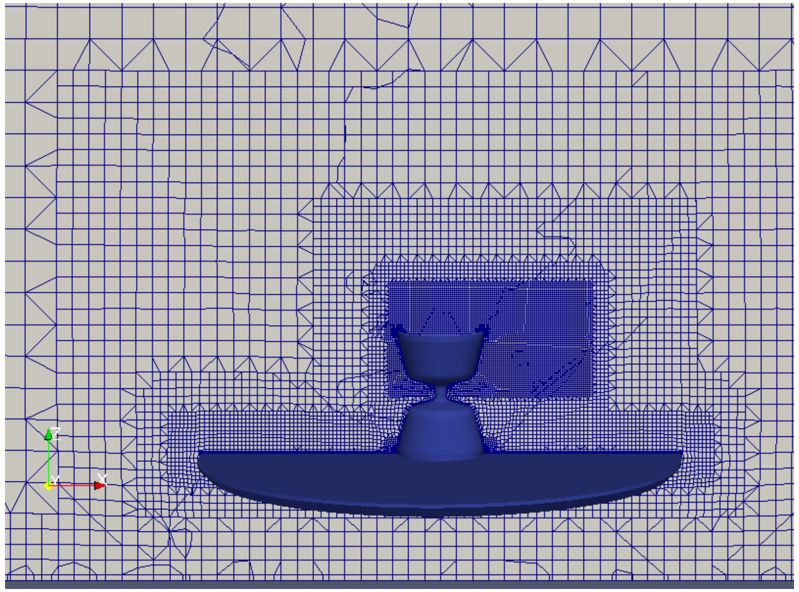

Mesh refined around the gauge, longitudinal section

2) turbulent base-flow

Solid fence upstream the gauge to generate the turbulent flow

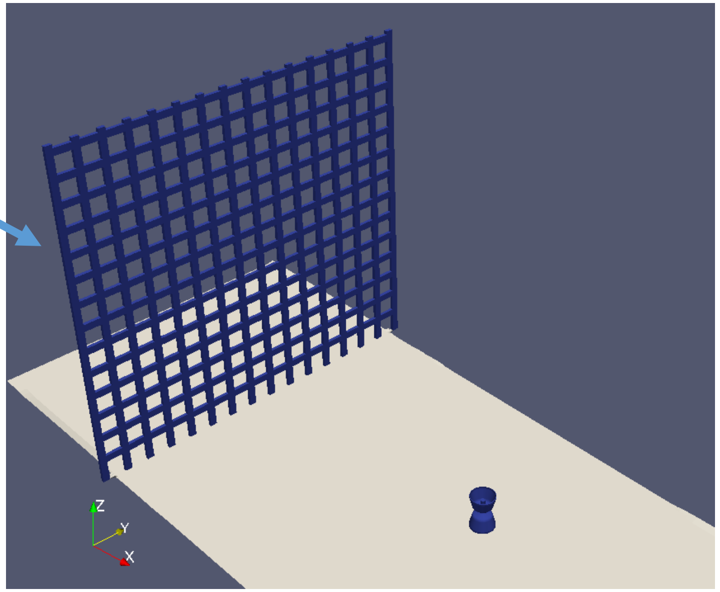

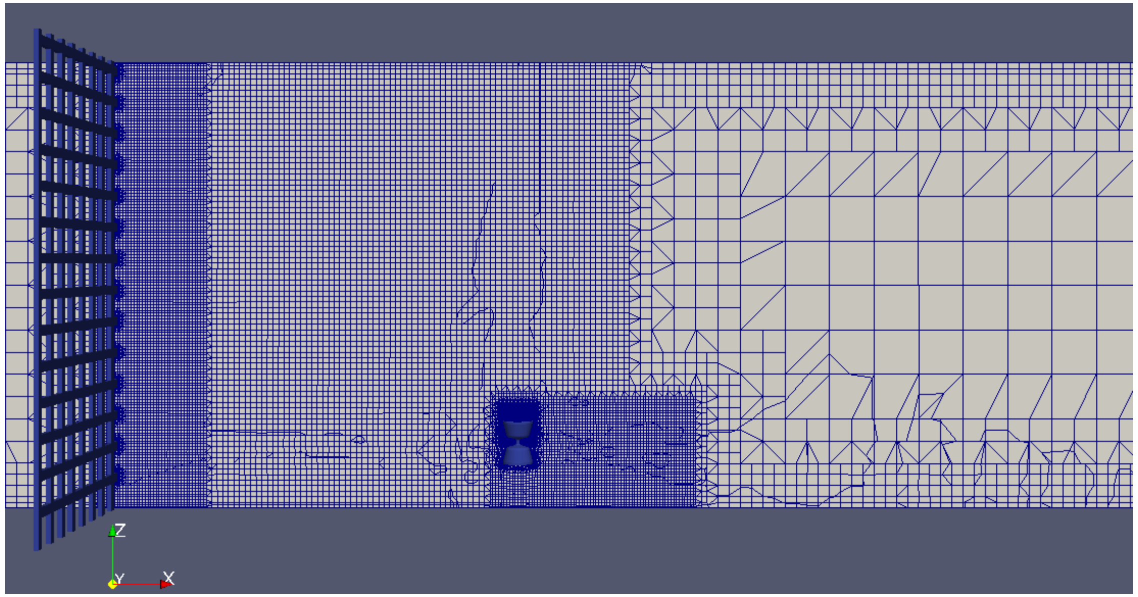

Some results

CFD flow fields

Uniform base flow | Turbulent base flow

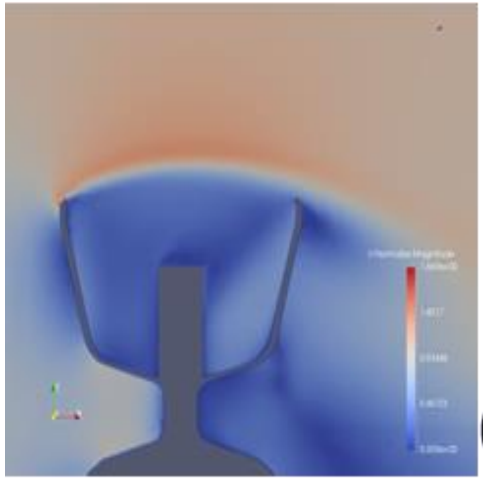
(a)
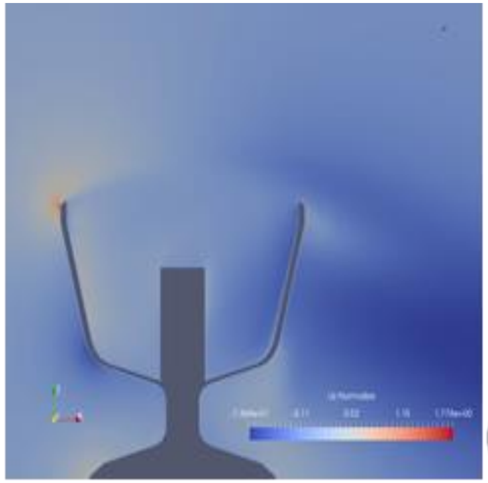
(b)
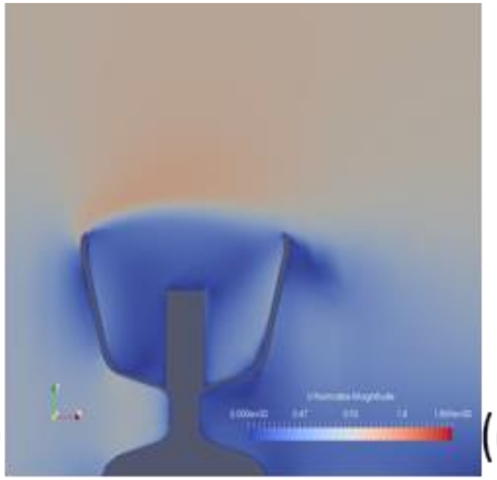
(c)
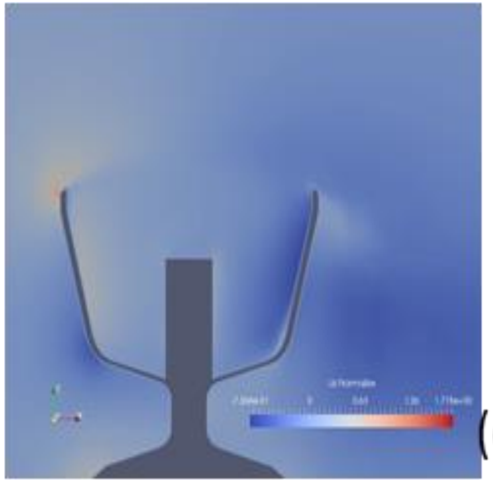
(d)

Normalized average flow velocity magnitude and vertical component

The turbulence base-flow velocity field and the updraft are lower than the uniform base flow case.

Wind tunnel setup


(a)
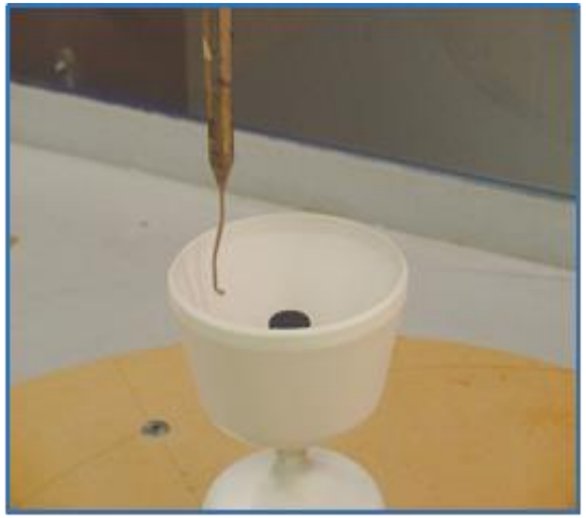
(b)

Some results

Vertical profile (a) of the velocity magnitude at the centre of the gauge (U_w=18ms^{-1})

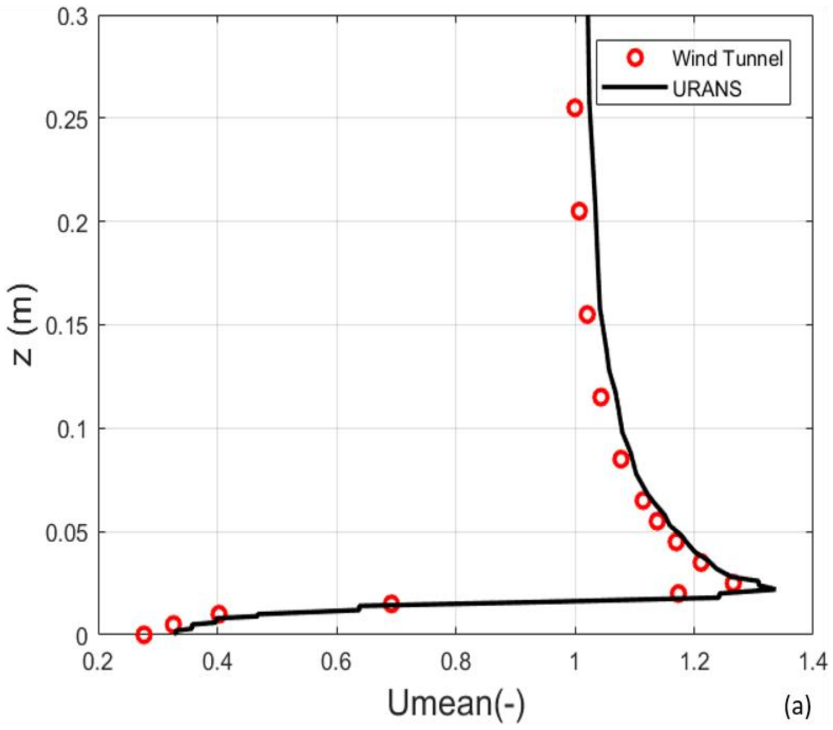

(a)

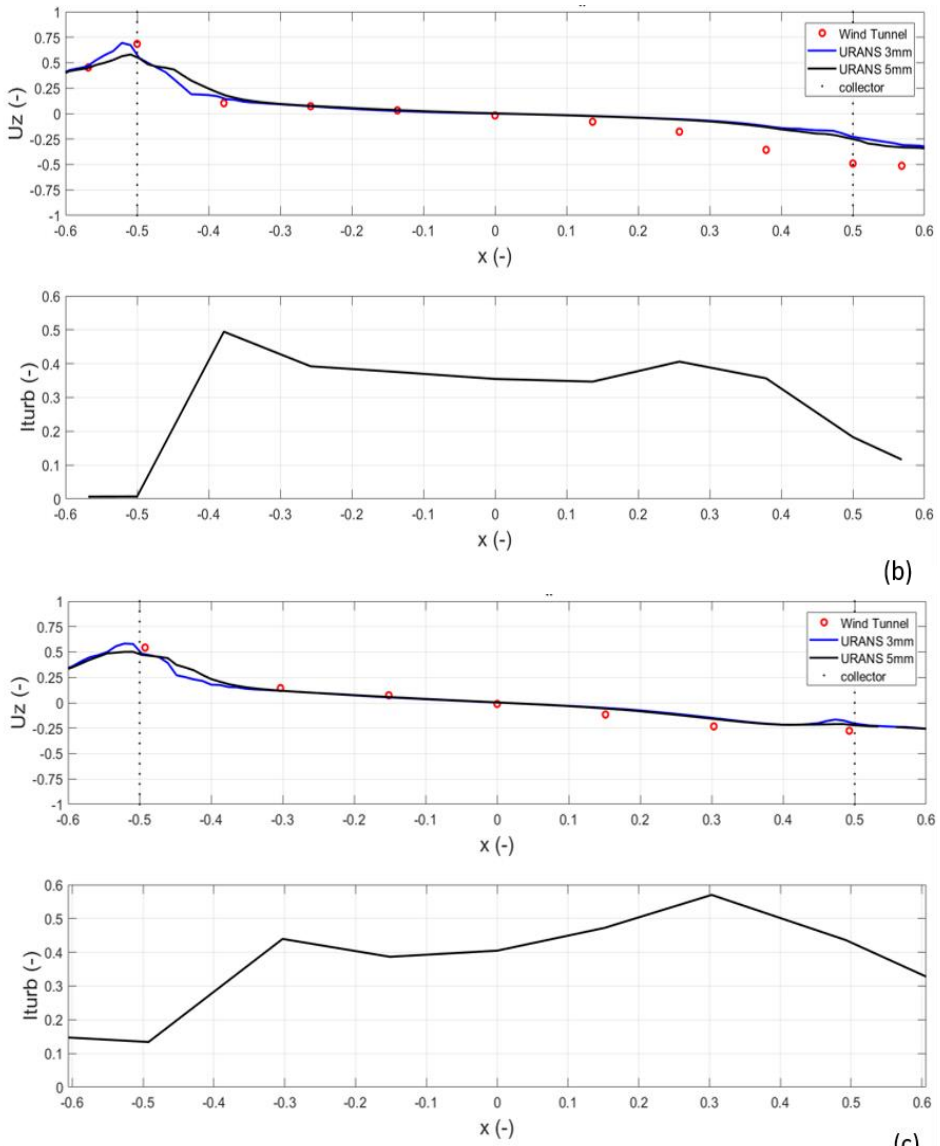

(b)

(c)

The longitudinal profiles of the vertical velocity component for the uniform (b) (U_w=18ms^{-1}) and turbulent (c) base flow (U_w=10ms^{-1}) above the collector, with the associated turbulence intensity profiles

Good agreement between WT measurements and CFD results

Further developments

- Better understanding of the role of turbulence on precipitation trajectories using LES simulations.
- Evaluation of the influence of the base flow turbulence on the precipitation trajectories.
- Use of a coupled approach to introduce the dispersed phase (liquid/solid particles) to evaluate the wind induced under-catch.
- Derive suitable correction curves for operational use.
- Validation of numerical results by means of wind tunnel flow measurements and CE field data.

THANK YOU FOR YOUR ATTENTION!

for further information:

http://www.precipitation-intensity.it

arianna.cauteruccio@edu.unige.it
luca.lanza@unige.it